AFPS – CFMS
Liquéfaction des sols sous séisme
CNAM Amphi C

Paris, 24 mars 2010

Retours d'expériences anciens et récents

P. MOUROUX

Liquéfaction – Retours d’expériences

1 - Les années 1964-1975

Rapport sur le glissement du

Lower San Fernando Dam (1973)

Séisme du 9 février 1971 – M=6.6

Lower San Fernando Dam

Séisme du 9 février 1971 – M=6.6

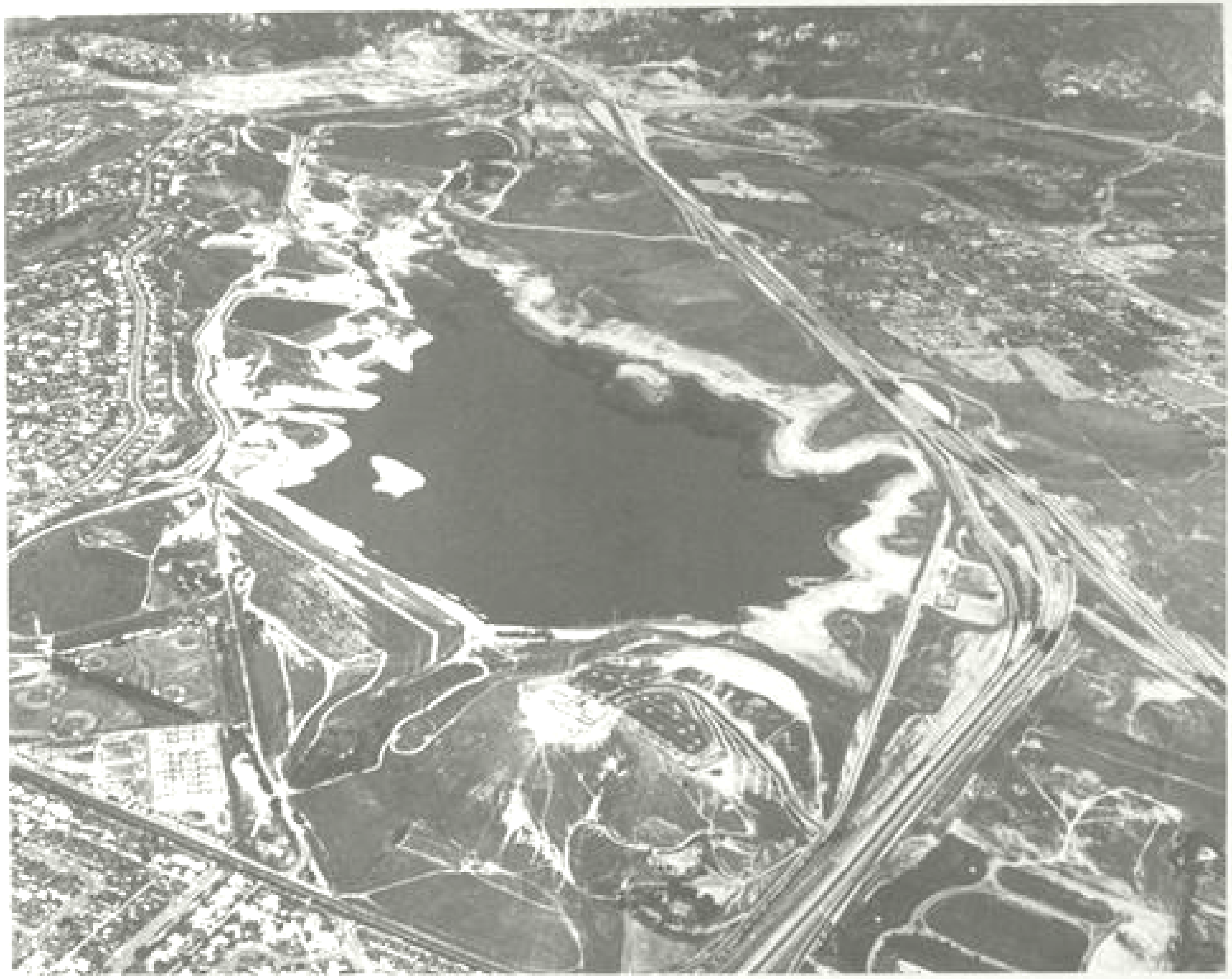

FIG. 1-1 AERIAL VIEW OF VAN NORMAN LAKE COMPLEX TAKEN AFTER EARTHQUAKE.
(Photograph by Department of Water Resources)

Lower San Fernando Dam

Séisme de San Fernando,

9 février 1971 – M=6.6

Barrage de 42m de hauteur

Remblai hydraulique

Glissement amont avec 1.5 m de revanche finale

80 000 personnes à l'aval immédiat,

très rapidement évacuées

Lower San Fernando Dam

Séisme du 9 février 1971 – M=6.6

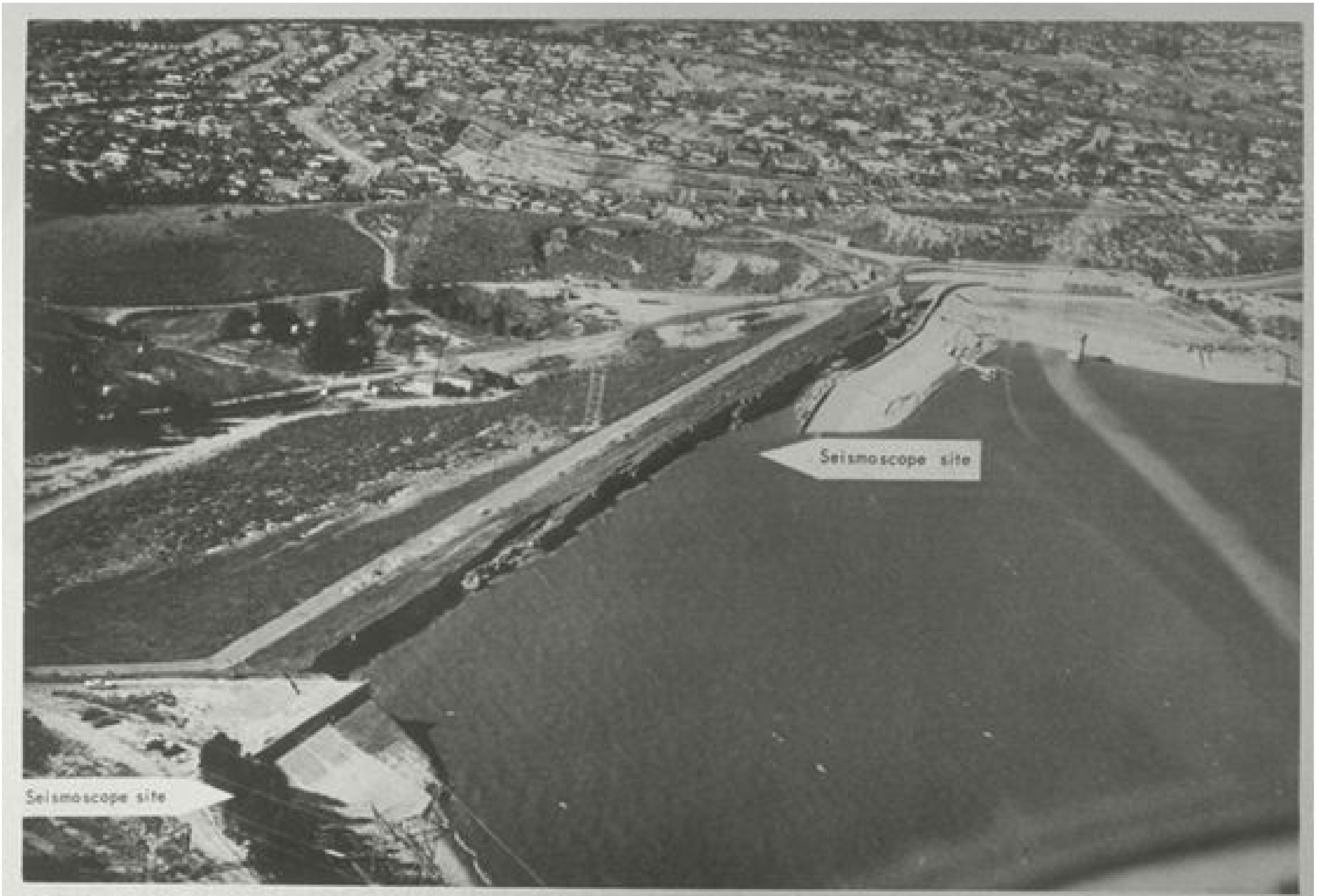

FIG. III-2 AERIAL VIEW OF LOWER SAN FERNANDO DAM AFTER EARTHQUAKE OF FEBRUARY 9, 1971. ARROWS INDICATE SEISMOSCOPE SITES. THE CREST SITE WAS COMPLETELY SUBMERGED FOLLOWING THE EARTHQUAKE.

(Photogragh by U.S. Geologic Survey)

Lower San Fernando Dam

Séisme du 9 février 1971 – M=6.6

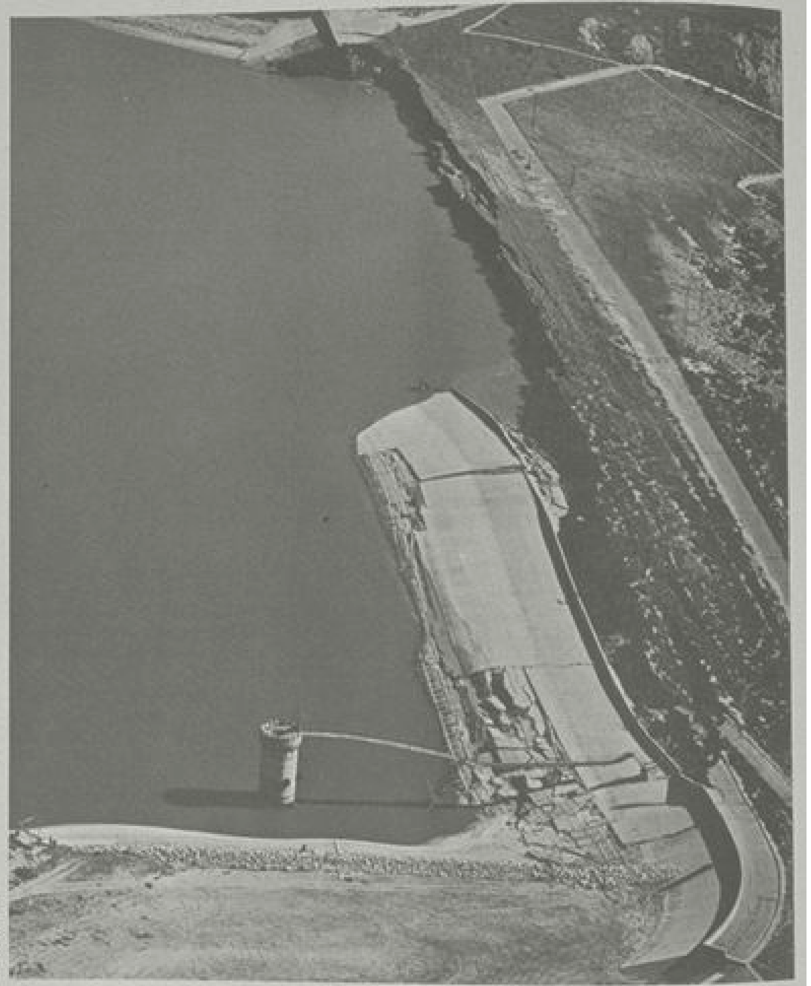

This aerial photo, taken on February 10, shows the extent of the damage to the hydraulic earth-fill dam on Lower Van Norman Reservoir. A large piece of the upstream face collapsed and fell into the water. The structure still standing was badly cracked (water oozing through the cracks is visible near the top of the photo). Fortunately, the water level was several feet below normal at the time of the quake, or even the damage here would have resulted in flooding of the residential areas below the reservoir.

Lower San Fernando Dam

Séisme du 9 février 1971 – M=6.6

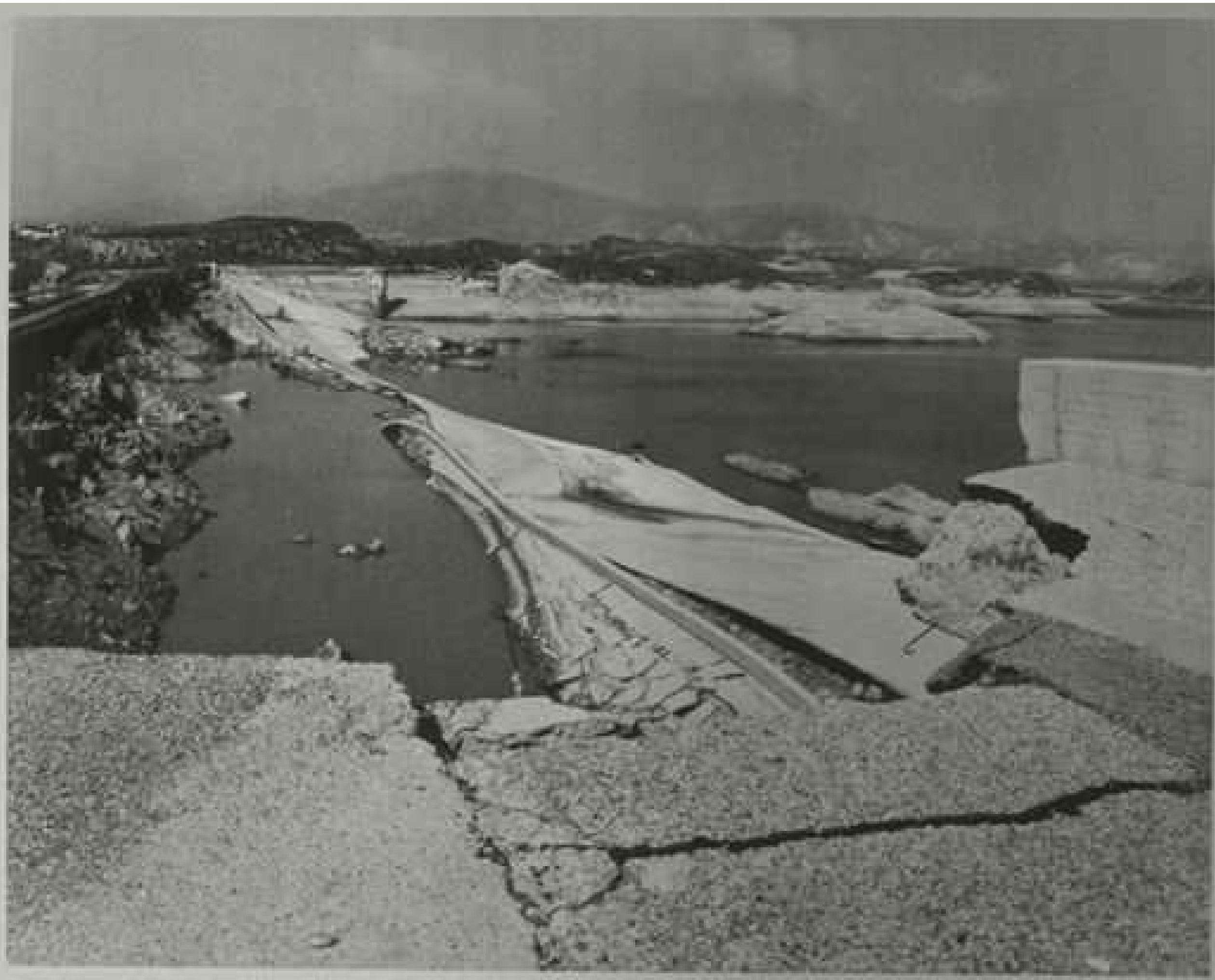

FIG. III-17 SLIDE DAMAGE TO LOWER SAN FERNANDO DAM.
(Photograph by Department of Water Resources, Feb. 22, 1971)

Lower San Fernando Dam

Séisme du 9 février 1971 – M=6.6

FIG. III – 18 SLIDE DAMAGE NEAR WEST ABUTMENT – LOWER SAN FERNANDO DAM

FIG. III–19 CENTRAL OUTLET TOWER – LOWER SAN FERNANDO DAM

FIG. III – 21 PILE–SUPPORTED FOOTING FOR BRIDGE TO CENTRAL OUTLET TOWER – LOWER SAN FERNANDO DAM

FIG. III – 22 SLIDE DEBRIS – LOWER SAN FERNANDO DAM

Questions posées :

+ Le glissement est-il en partie dans la fondation ou uniquement dans le remblai ?

+ Quelle est la mécanique du glissement ?

+ Pouvait-on l'anticiper ?

+ Quels nouveaux critères pour évaluer la sécurité des barrages ?

Travaux réalisés :

+ Grandes tranchées au sein du massif

+ Très nombreux essais de laboratoires et in situ :

résistance à la liquéfaction.

+ Reconstitution du mécanisme du glissement

+ Analyse classique pseudo-statique

+ Analyse dynamique nouvelle :

* Contraintes initiales dans le barrage (Duncan : Isbild)

* Mouvement sismique,

* Réponse dynamique du barrage, pas à pas dans le temps (Seed, Idriss, etc..: Quad 4) et comparaison avec contraintes nécessaires pour avoir liquéfaction.

* Mise en évidence des zones ayant pu liquéfier

Lower San Fernando Dam

Reconstitution du glissement

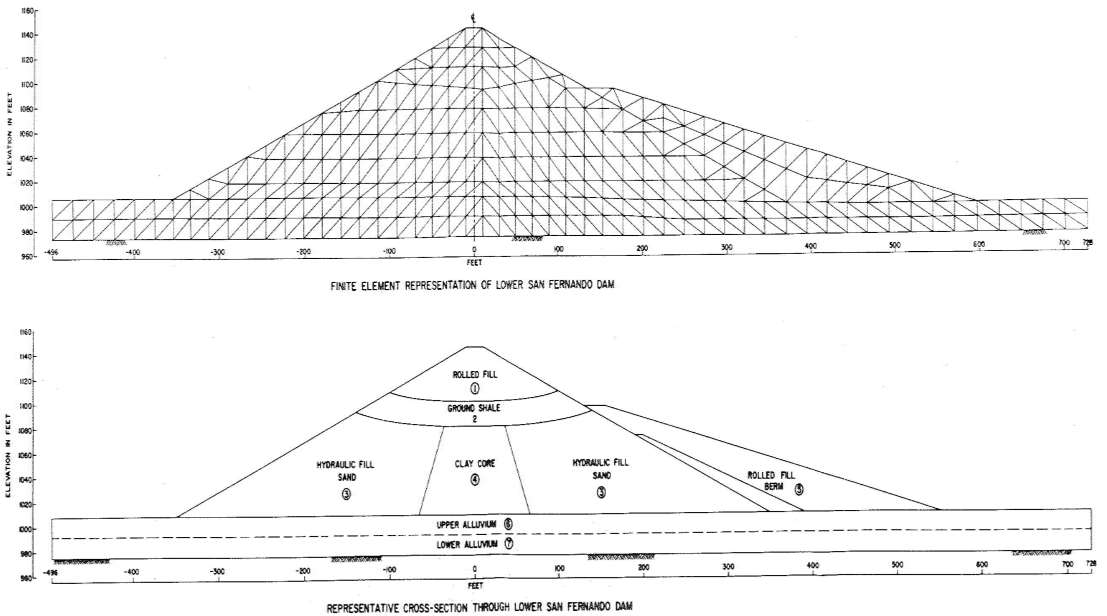

Fig. VIII-2 CROSS-SECTION THROUGH LOWER SAN FERNANDO DAM USED FOR DYNAMIC ANALYSIS

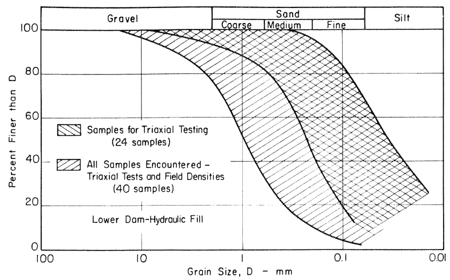

Fig. V-23 RANGES OF GRAIN SIZE DISTRIBUTION CURVES FOR HYDRAULIC FILL – LOWER SAN FERNANDO DAM.

Lower San Fernando Dam

Reconstitution du glissement

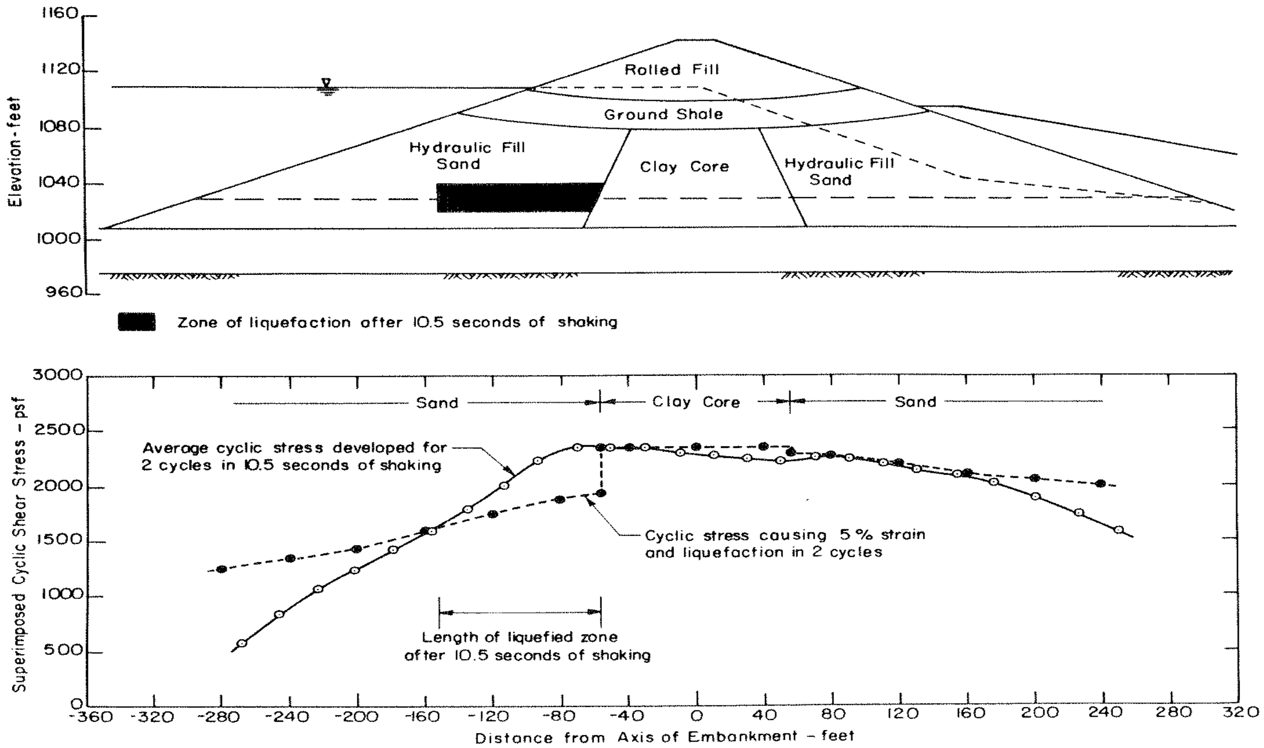

Fig. VIII–7 ANALYSIS OF SOIL STABILITY ALONG PLANE AT ELEVATION 1030 FT. AFTER 10.5 SECONDS OF SHAKING, USING BASE MOTIONS DETERMINED FROM SEISMOSCOPE RECORD – LOWER SAN FERNANDO DAM.

Lower San Fernando Dam

Reconstitution du glissement

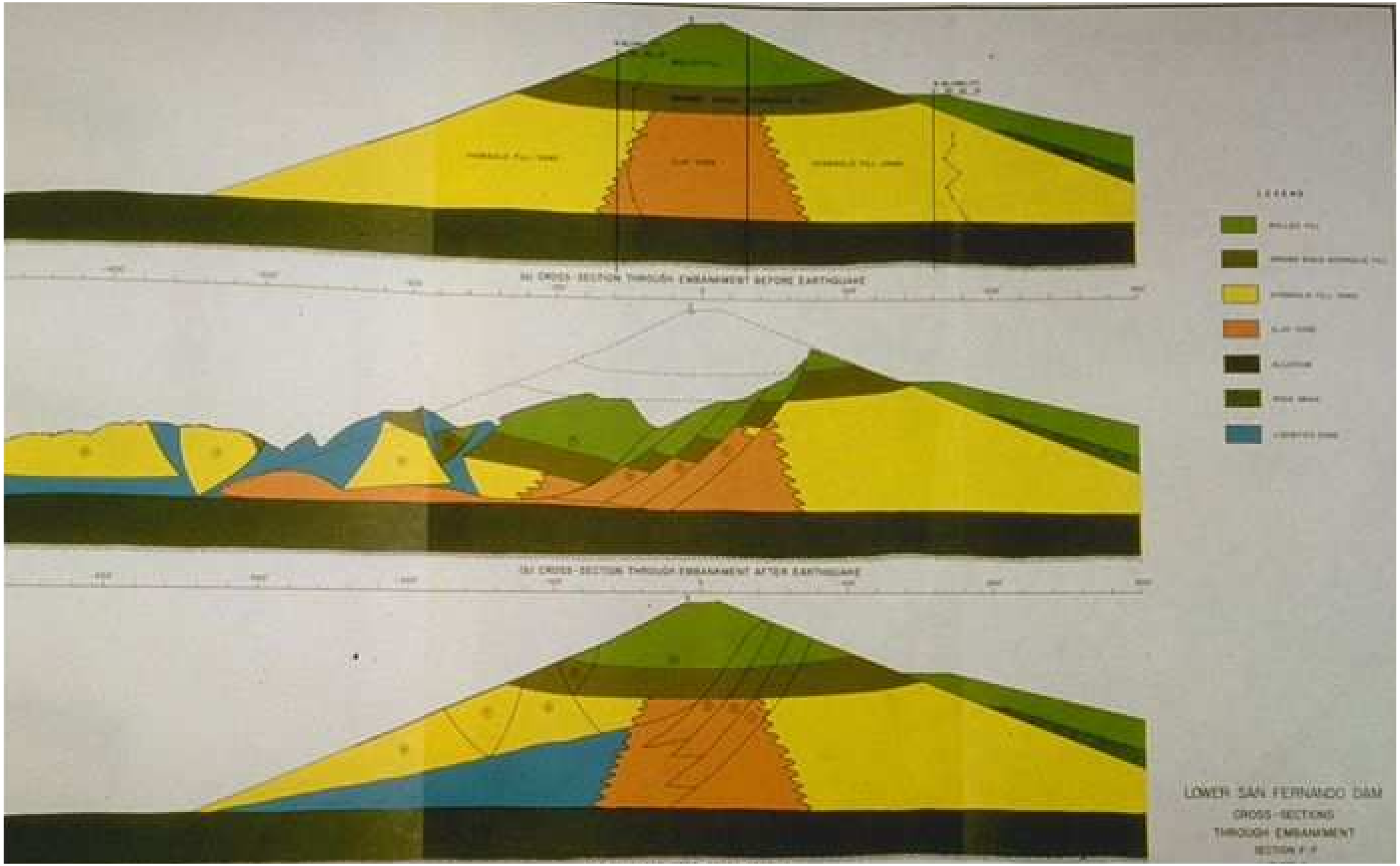

1964 – Niigata - Japon

Liquéfaction en zone alluviale

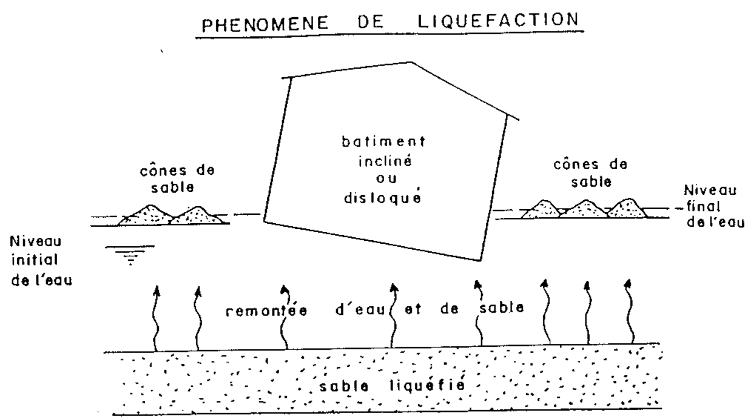

Séisme de Niigata, le 16 juin 1964

+ M=7.5 Epicentre à 22 km de la côte, Foyer à 40 km de profondeur

+ amax enregistrée, de 0.08 à 0.25 g

+ Plus de 2000 bâtiments inclinés, dans une zone alluviales,

avec très mauvaises caractéristiques mécanique, N < 10,autour de 6 à 10m de profondeur

+ 28 morts au total seulement !!

+ Importance des déplacements horizontaux, près de la rivière Shinano, jusq'à 12 m, avec dommages généralisés aux canalisations :

Etude en retour de Hamada et O'Rourke, en 1992,

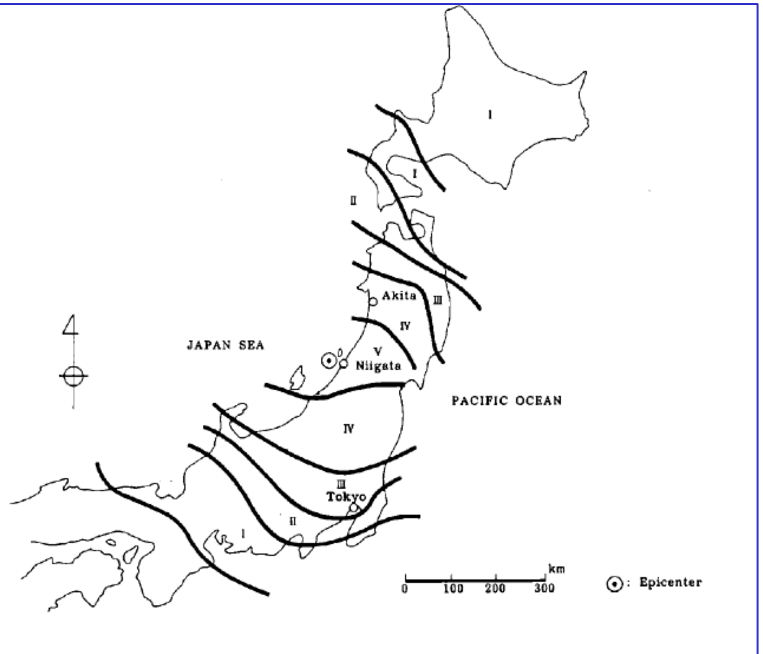

Figure 1. Epicenter and Seismic Intensity (JMAI) of the 1964 Niigata Earthquake[2)]

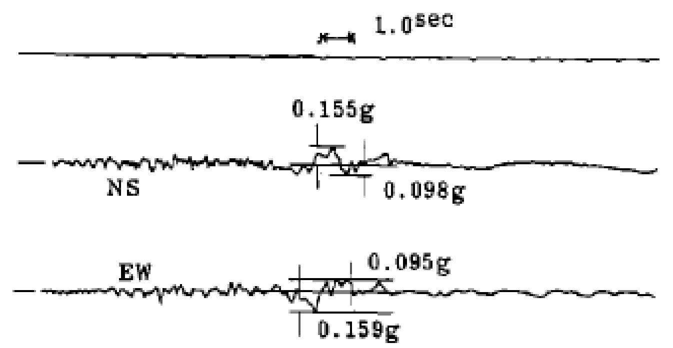

(a) In The Basement

1964 – Niigata - Japon

Liquéfaction en zone alluviale

1964 – Niigata - Japon

Liquéfaction en zone alluviale

1964 – Niigata - Japon

Liquéfaction en zone alluviale

1964 – Niigata - Japon

Liquéfaction en zone alluviale

1964 – Niigata - Japon

Liquéfaction en zone alluviale

1964 – Niigata - Japon

Liquéfaction en zone alluviale

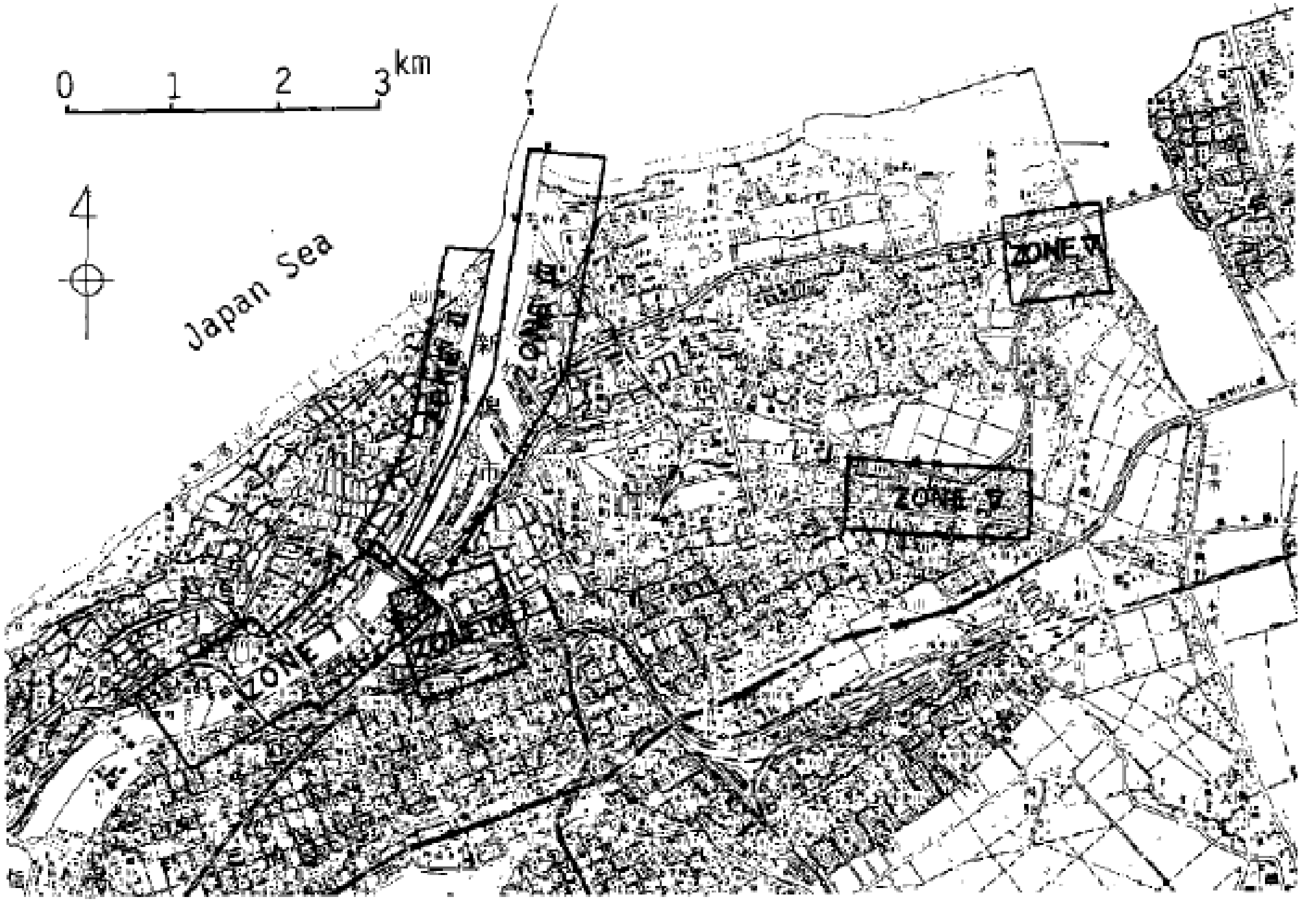

Figure 4. Six Zones for Measurement of Permanent Ground Displacements in Niigata City

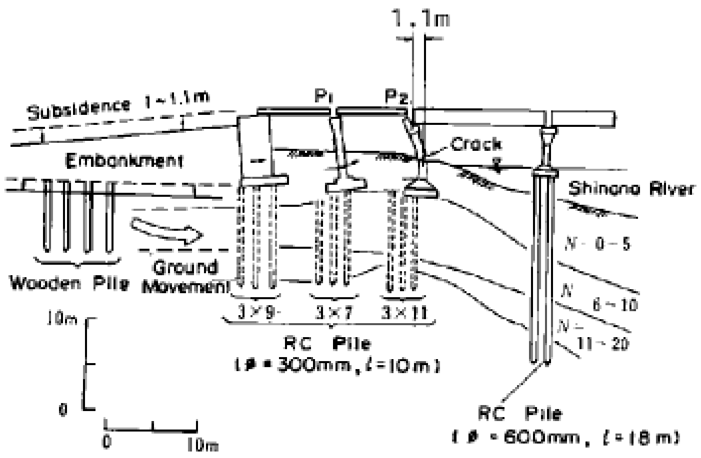

Figure 9. Damage to Yachiyo Bridge[5),6)]

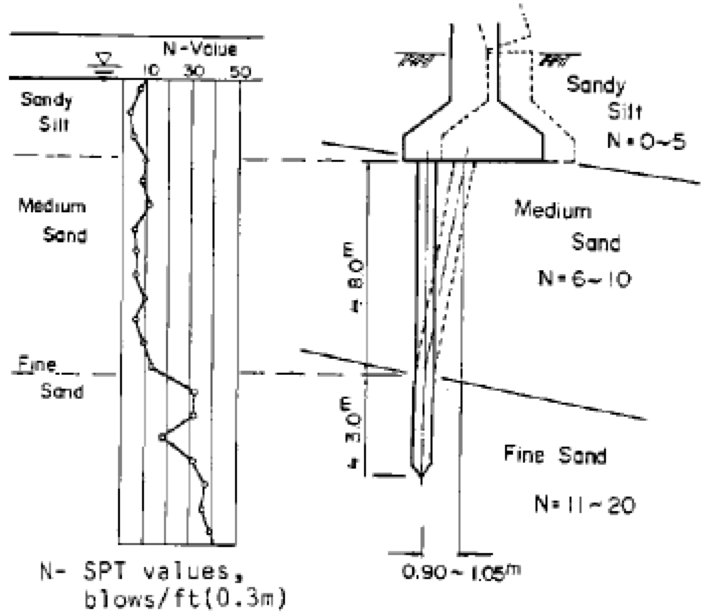

Figure 10. Damage to a Foundation Pile of Yachiyo Bridge(P_2)[7)]

1964 – Niigata - Japon

Liquéfaction en zone alluviale

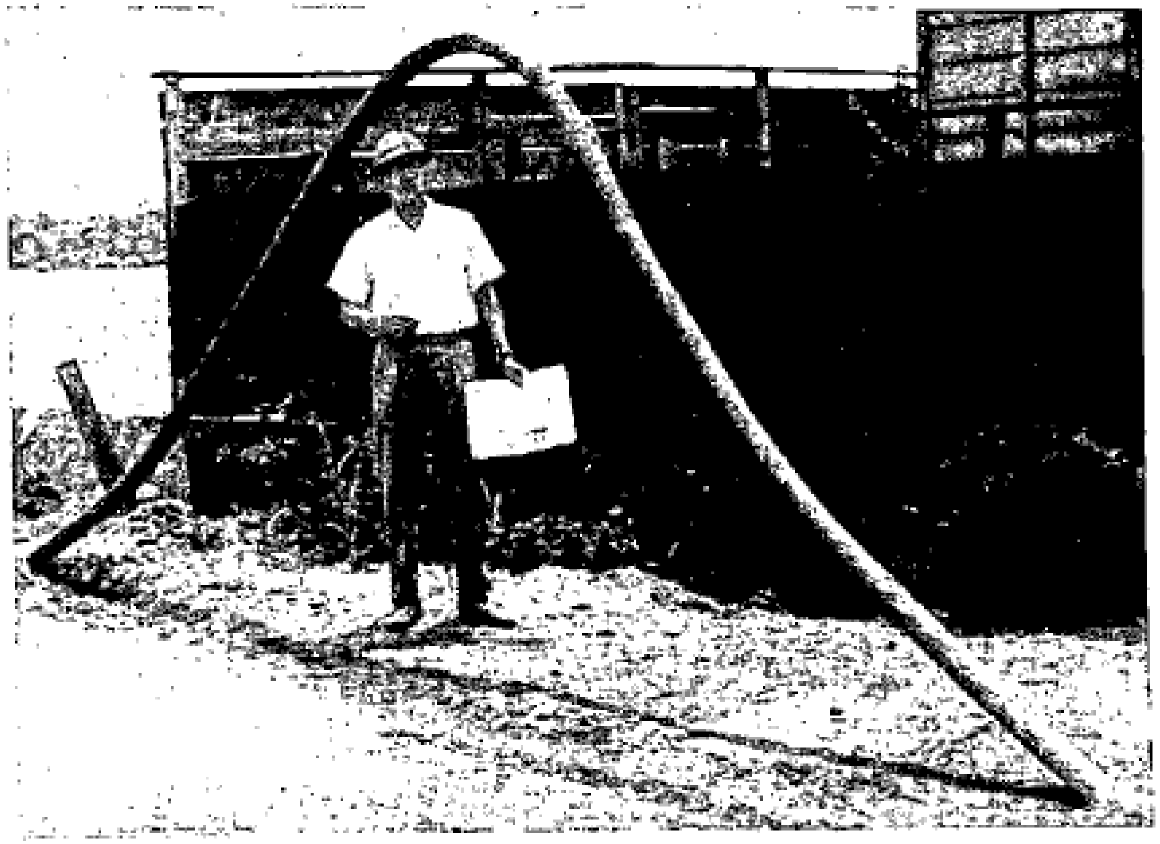

Photo 31 Buckling of a Buried Gas Pipe

Séisme d’ Alaska, le 27 mars 1964

+ Mw =9.2 Subduction + Tsunami

+ Liquéfaction classique

+ Liquéfaction en bordure de pente marine et terrestre:

Anchorage -Turnegain Heights, L-Street, …….

+ 131 morts au total !!

1964 – Alaska

Liquéfaction classique et en bordure de pente

Glissement Turnagain Heights

Glissement Turnagain Heights

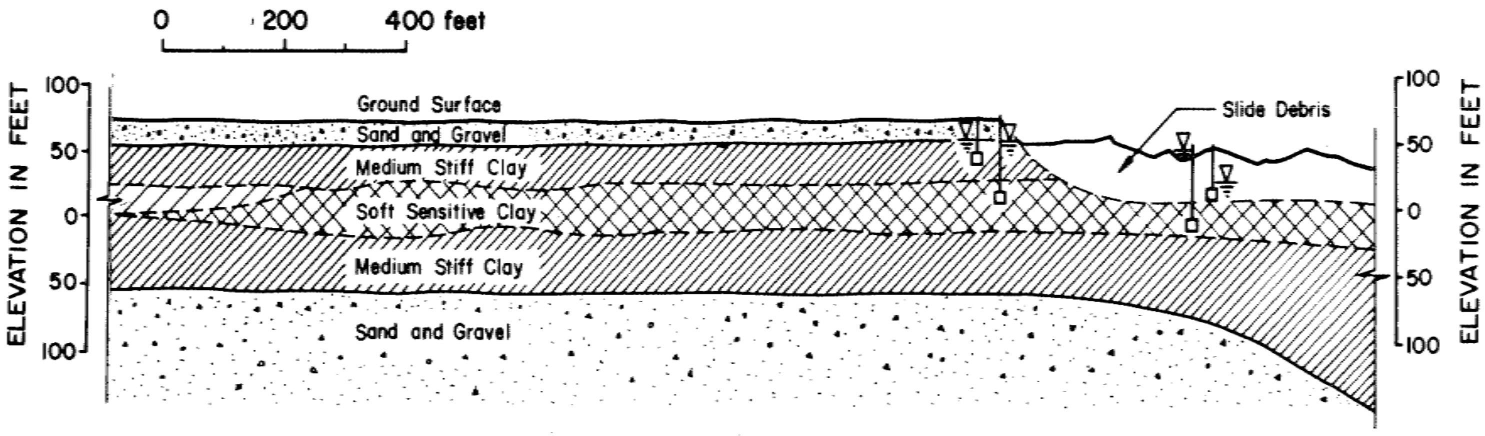

Fig.44-SECTION THROUGTH EAST END OF TURNAGAIN HEIGHTS SLIDE AREA, ANCHORAGE (1964).

1964 – Alaska

Liquéfaction classique et en bordure de pente

Glissement Turnagain Heights

1964 – Alaska

Liquéfaction classique et en bordure de pente

Glissement L-Street

Fig. 33 - GRABEN BEHIND 'L-STREET' SLIDE AREA, ANCHORAGE (1964).

Fig. 34 – AERIAL VIEW OF GRABEN BEHIND 'L-STREET' SLIDE AREA, ANCHORAGE (1964).

(U.S. Army Photograph)

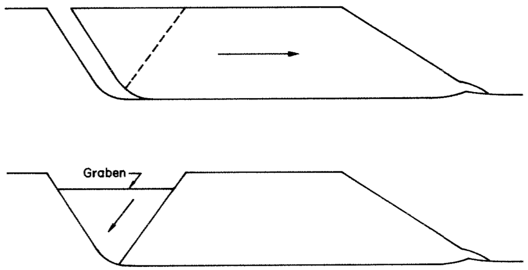

Fig. 32 - MECHANISM OF GRABEN FORMATION DUE TO SLIDING ON HORIZONTAL LAYER.

1964 – Alaska

Liquéfaction classique et en bordure de pente

Glissement L-Street

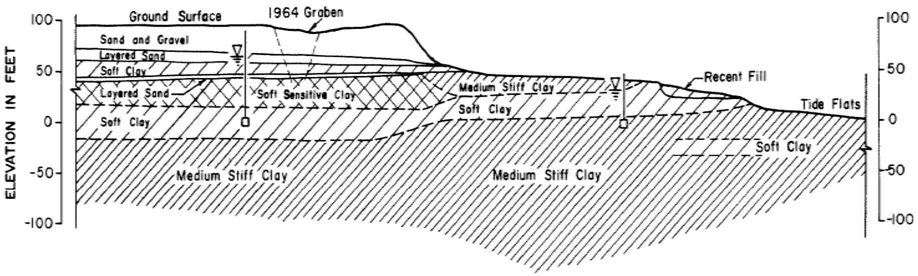

Fig. 35 - SOIL CONDITIONS IN L-STREET SLIDE AREA, ANCHORAGE.
(After Shannon and Wilson)

Fig. 36 - UNDAMAGED HOUSES ALONGSIDE GRABEN, L-STREET SLIDE AREA, ANCHORAGE (1964).

Fig. 39 - DIFFERENTIAL SETTLEMENT OF BUILDING AT EDGE OF GRABEN, ANCHORAGE (1964).

Glissement Lac Rinihue (Chili) - 1960

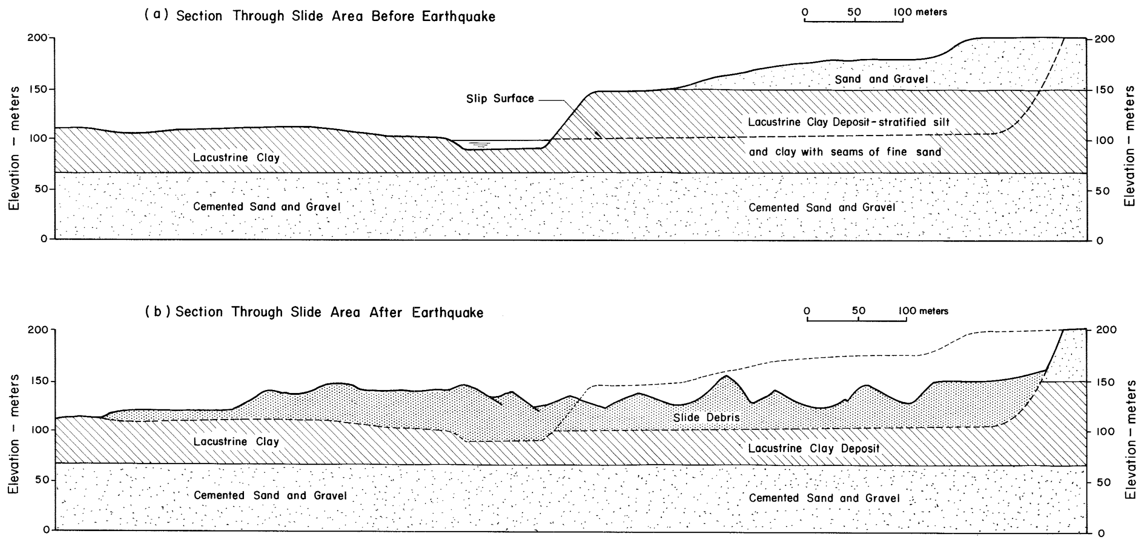

Fig. 49 – APPROXIMATE SECTIONS THROUGH LARGE SLIDE AREA NEAR LAKE RINIHUE, CHILE (1960).

(After Davis and Karzulovic)

Liquéfaction – Retours d’expériences

1 - Les années 1964-1975

Très nombreuses recherches, en particulier à Berkeley, Caltech, MIT, au Japon, etc..

Dont :

+ Méthode simplifiée liquéfaction:

Seed-Idriss (EERC : 1970)

+ Programmes de base pour l’analyse dynamique : Shake1D, Isbild, Quad 4, ………

+ Observations et retours d’expérience

Liquéfaction – Retours d’expériences

2 – Avant 1964

+ Helike : 373 BC

+ Jamaïque : 1692

+ Cascadia-Vancouver- Seattle : 1700

+ New Madrid : 1811-1812

+ L’année 1906 : San Francisco,

Valparaiso, Temuco (Equateur)

+ Japon : 1891 (Nobi),

1923 (Kanto-Tokyo),

1948 (Fukui)

+etc…

Liquéfaction : Jamaïque - 1692

Evidence **he 1692 Port**
Royal, **uefaction.**

1906 – San Francisco

Liquéfaction en zones alluviale et marine + Remblais

San Francisco - 1906

1923 – Kanto - Japon

Liquéfaction en zone alluviale et marine + Remblais

1923 – Kanto – Japon, le 1er septembre 1923

M = 7.9 Liquéfaction observée jusqu'à plus de 100 km de l'épicentre

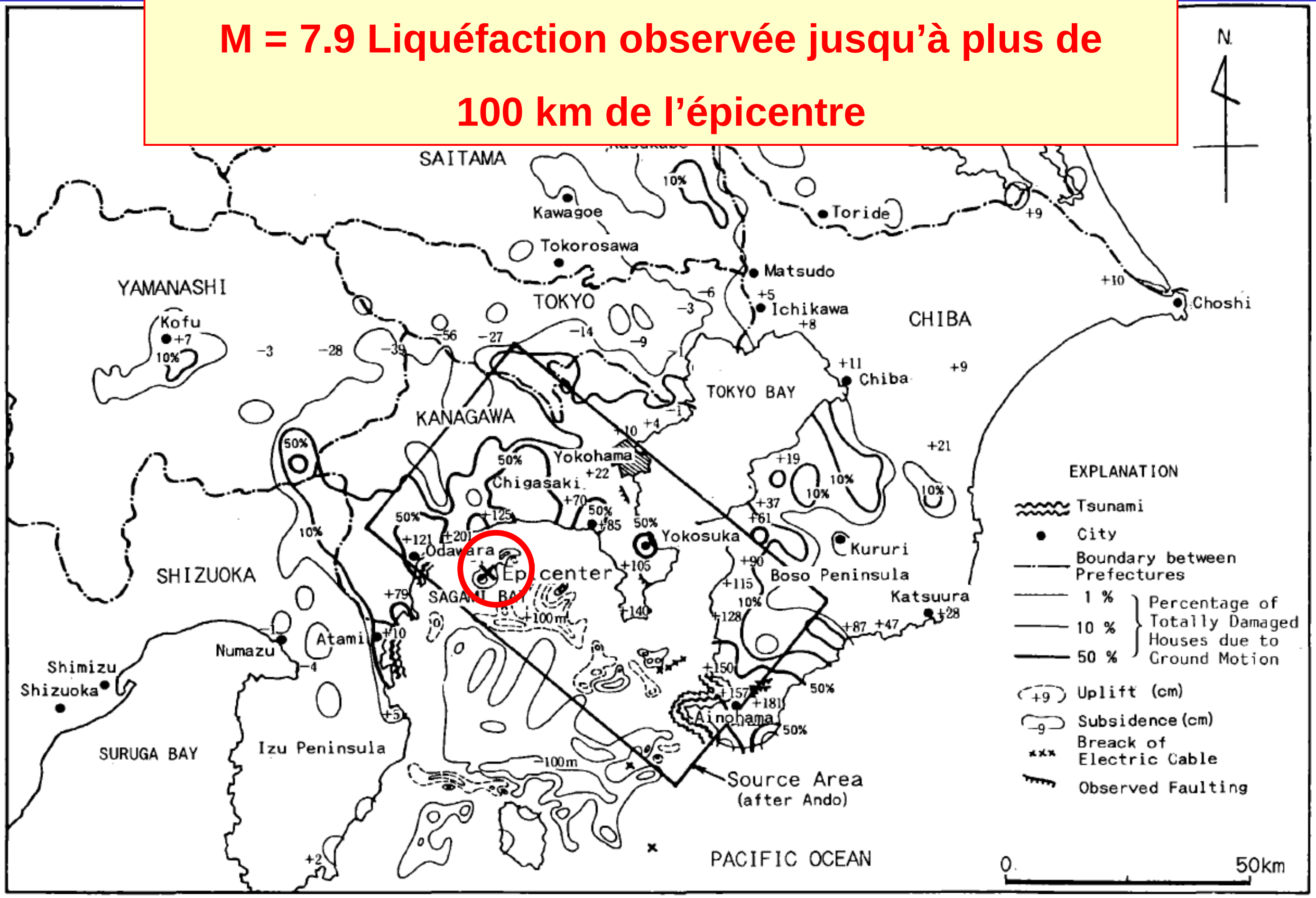

Figure 1 Map of Kanto and Chubu Districts Showing Distribution of Seismic Damage Caused by the 1923 Kanto Earthquake (Modified from Usami, 1987)[8]

Etude en retour de Hamada (1986) + O'Rourke, en 1992

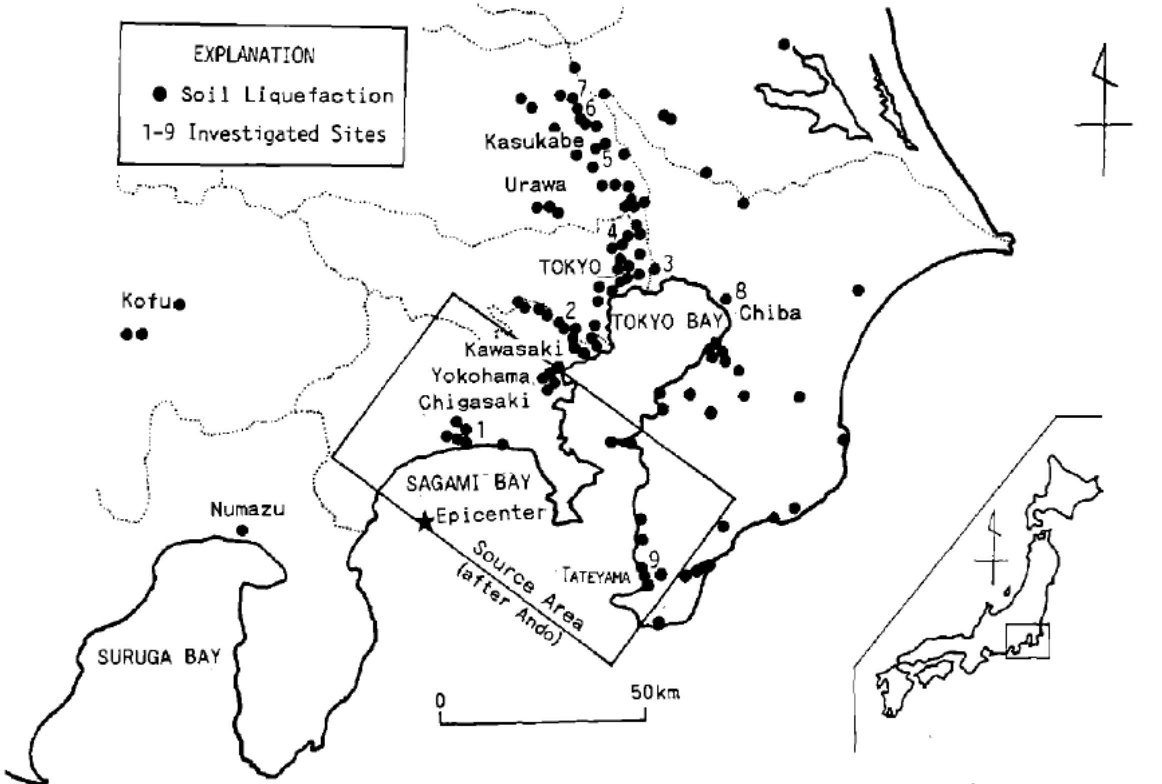

Figure 2 Map of Kanto and Chubu Districts Showing Principal Areas Affected by Liquefaction during 1923 Kanto Earthquake

1923 – Kanto - Japon

Liquéfaction en zone alluviale et marine + Remblais

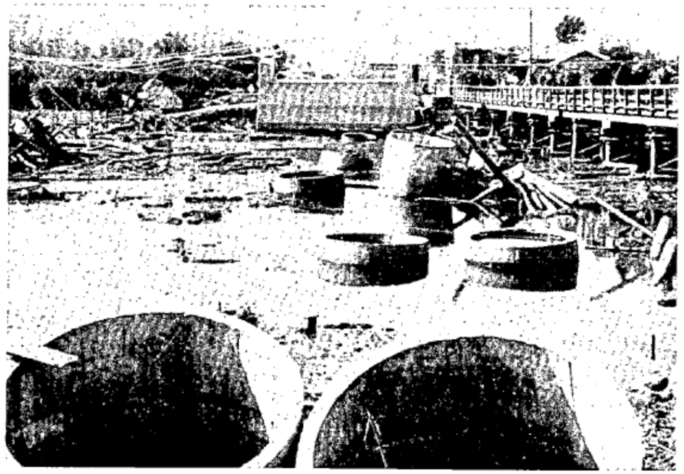

Figure 6 Tilting, Rising up and Lateral Movement of Open Caissons of Banyu Bridge over Sagami River (Japan Society of Civil Engineers, 1927)[12)]

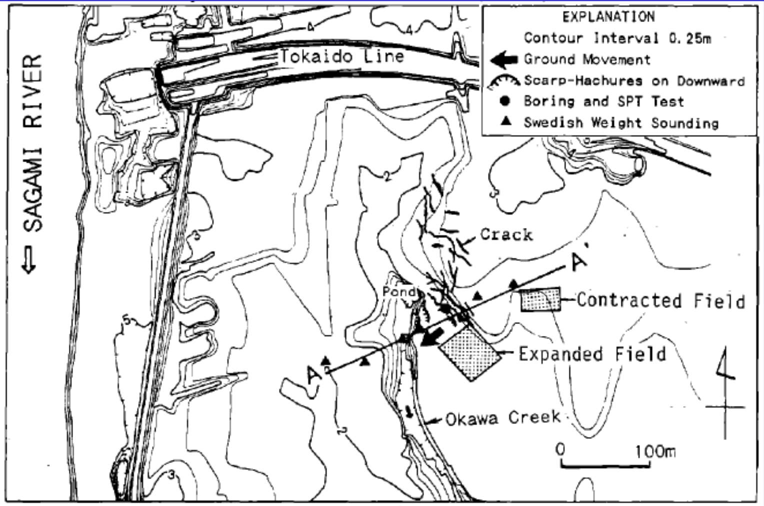

Figure 8 Contour Map of Nakajima Showing Locations of Ground Cracks and Ground Deformation Generated by Lateral Ground Movement and Location of Borings and Soundings for the Cross Section A-A' in Figure 12

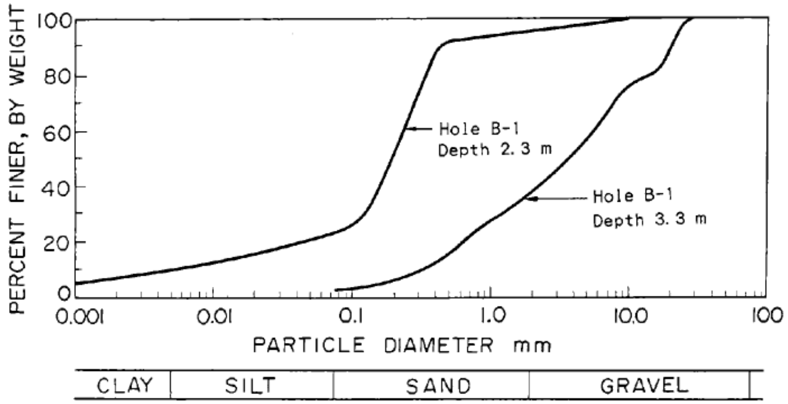

Figure 13 Grain Size Distribution Curves from Fine Sand Layer and Sandy Gravel Layer at Nakajima Area

1923 – Kanto - Japon

Liquéfaction en zone alluviale et marine + Remblais

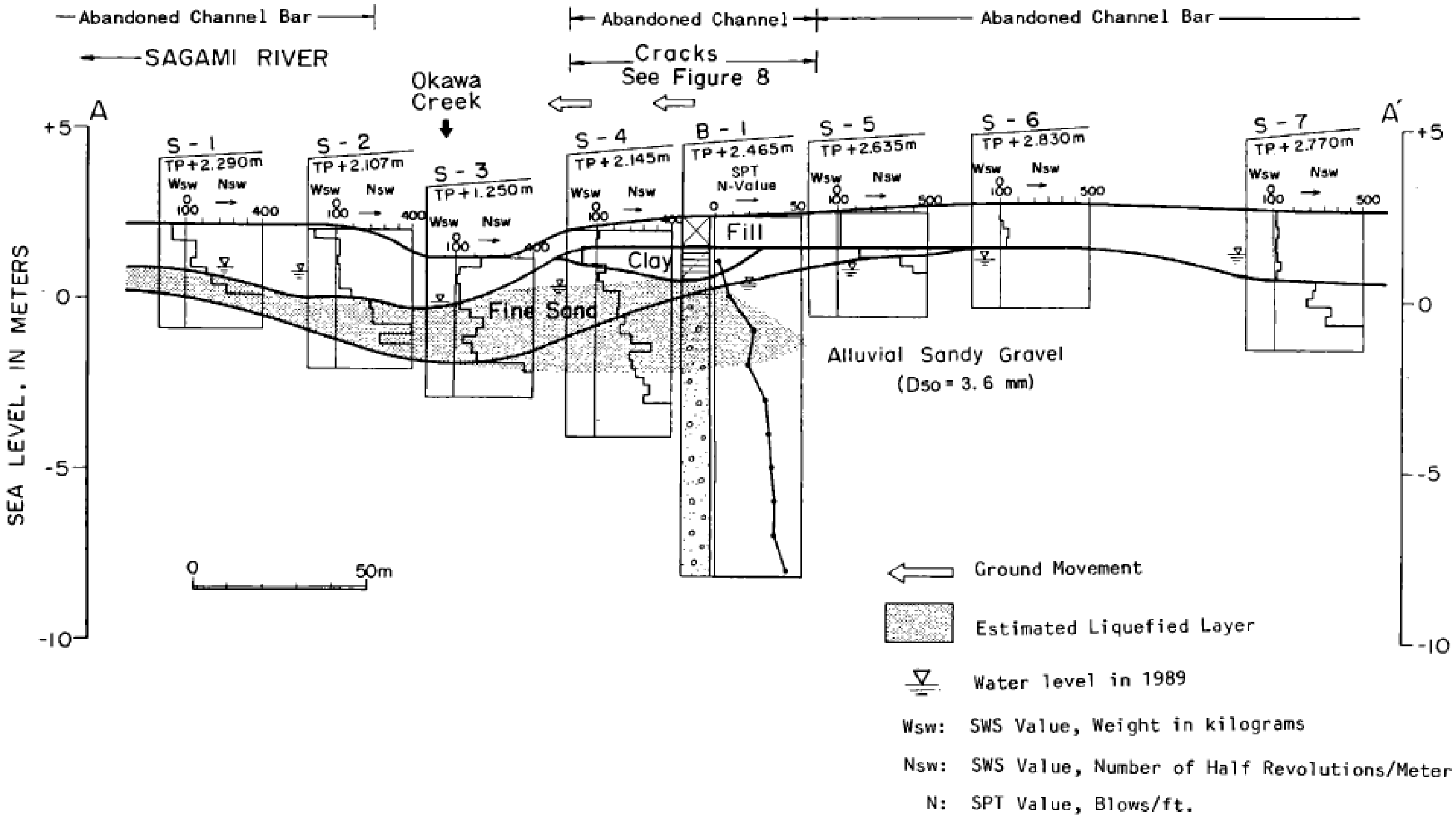

Figure 12 Cross Section of Sediments at Nakajima Area Showing Geotechnical Features and Estimated Liquefied Layer

1923 – Kanto - Japon

Liquéfaction en zone alluviale et marine + Remblais

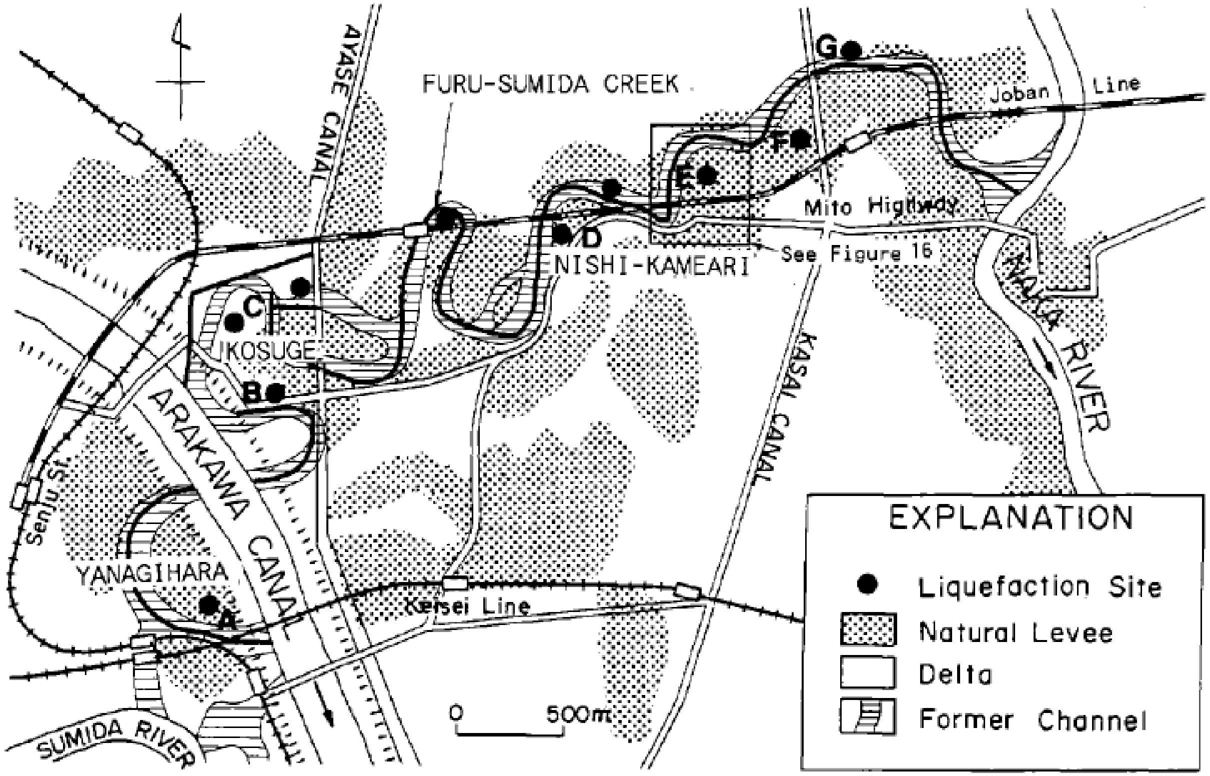

Figure 14 Map of Furu-Sumida Creek Area Showing Geographical and Geomorphological Features and Locations of Liquefaction

1923 – Kanto - Japon

Liquéfaction en zone alluviale et marine + Remblais

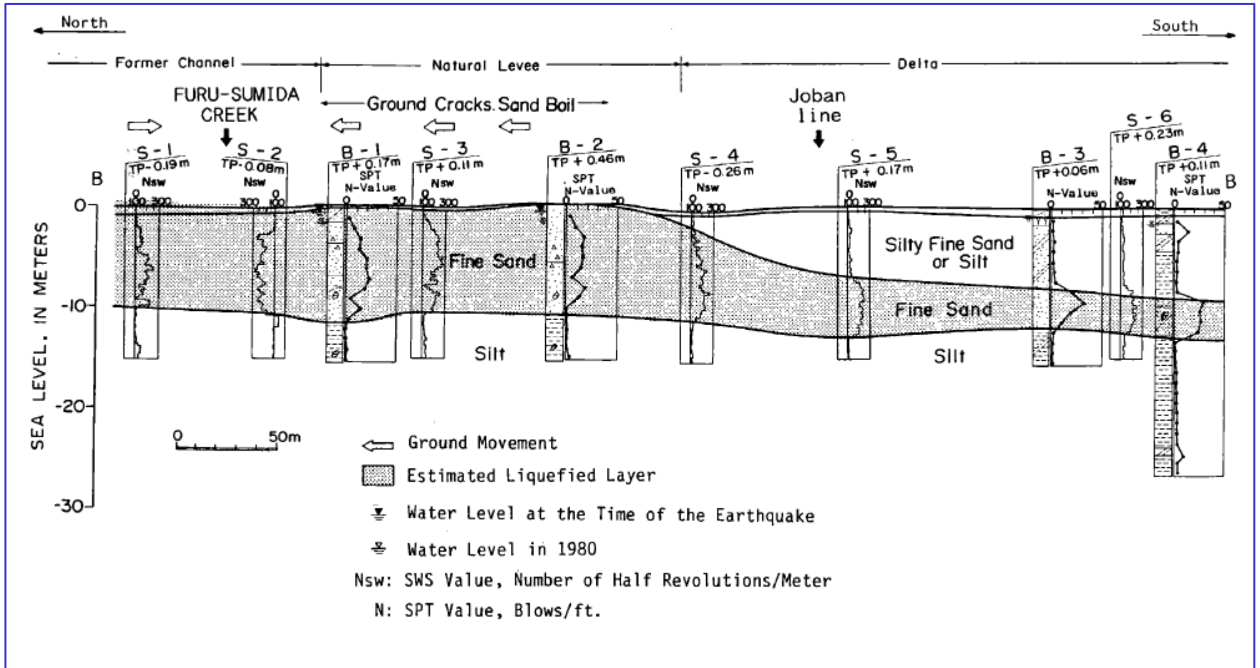

Figure 18 Cross Section of Sediments at Nishi-Kameari, Tokyo, Showing Geotechnical Features and Estimated Liquefied Layer

8.0 CONCLUSION

The following characteristics can be summarized from the case study of the liquefaction-induced ground failures and their related damage to structures during the 1923 Kanto earthquake:

(1) Liquefaction-induced ground failures occurred widely in many locations in the Tokyo Metropolitan area during the 1923 Kanto earthquake. The most distant location is about as far away as 150 km northeast of the epicenter.

(2) Three areas were identified where large horizontal ground displacement had been induced by the earthquake. The magnitude of the permanent displacement was estimated to be as large as several meters.

(3) The ground displacements occurred from a topographically higher site such as natural levees and former channel bars toward small rivers. These rivers were only several meters wide at the time of the earthquake but had been much wider a few centuries before the earthquake.

(4) Typically, the ground surfaces at displacement sites are inclined slightly toward the direction of ground movements. The surface gradients generally are very small, being less than 1%.

(5) The ground water levels at the sites are 0.5 m-2.0 m below the ground surface, according to recent bore hole data, and are inclined slightly in the direction of observed ground movements.

(6) The depth and extent of the liquefied layers were identified by the procedure of the Japanese Highway Bridge Code as well as a comparison between soil ejected during the earthquake and samples from the bore holes. The characteristics of the liquefied layers can be summarized as follows:

1923 – Kanto - Japon

Liquéfaction en zone alluviale et marine + Remblais

(i) Upper boundaries of the estimated liquefied soil layers are at a depth 0.3-2 m below the ground surface and are slightly inclined in the direction of observed ground movements, consistent with the inclination of the ground surfaces and ground water levels.

(ii) The thickness of the estimated liquefied soil layers range from 3 m to a maximum of 11 m.

(iii) Grain size distribution curves of the samples taken from the Furu-Sumida Creek area and Kawakubo area show that they are clean, uniform and medium to fine sands. However, the samples from the Nakajima area of Chigasaki City are coarse and well drained. In this area, it is probable that the low permeability of the surface sediments promoted the development of excess pore water pressure of the underlying gravelly layers, thereby resulting in liquefaction and ground deformations.

(7) Sand boils recurred in several locations during successive large earthquakes. This fact indicates that sites of past liquefaction are likely to liquefy if soil and groundwater conditions remain unchanged.

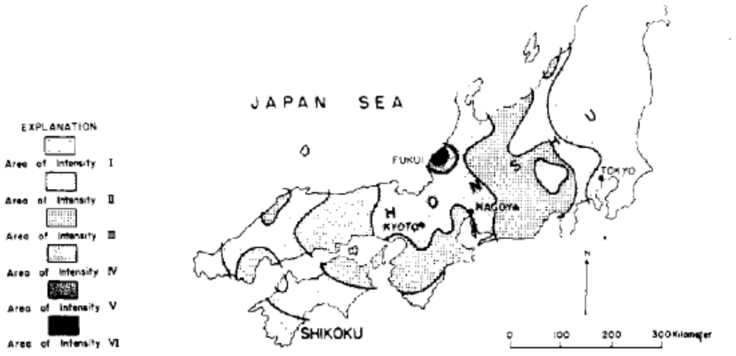

Figure 2. Seismic Intensity on Japan's Honshu Island (Japan Meteorological Agency Intensity Scale)[1]

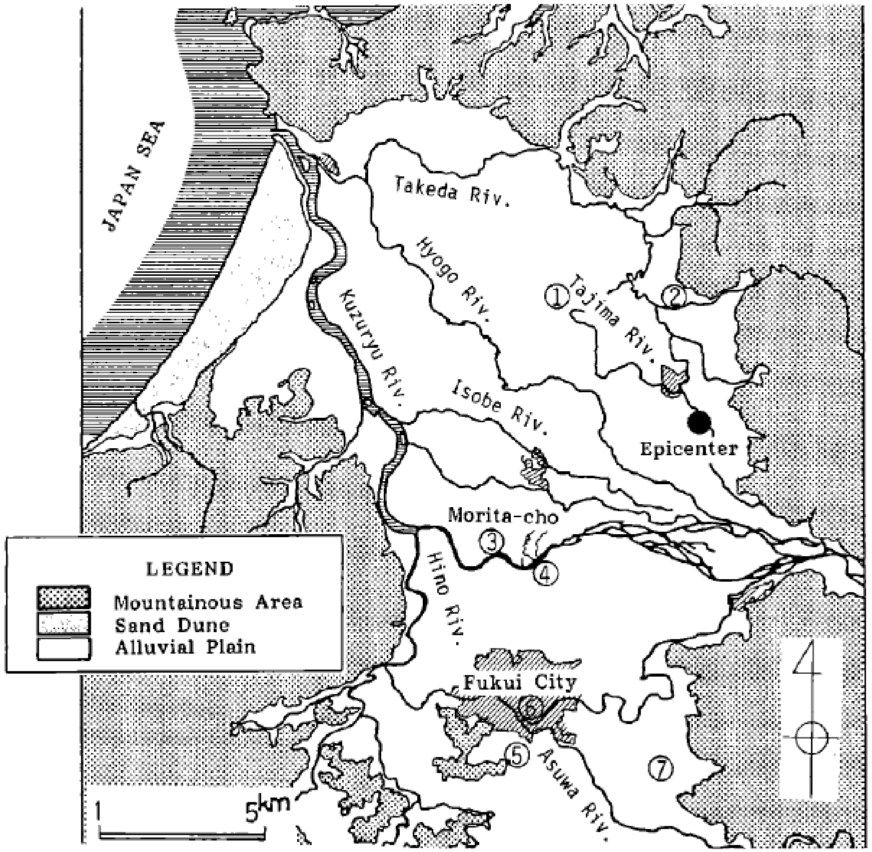

Figure 1. Fukui Plain and Epicenter of 1948 Fukui Earthquake

1948 – Fukui - Japon

M = 7.1, amax de 0.25 à 0.40 g

1948 – Fukui - Japon

Liquéfaction en zone alluviale

Etude en retour de Hamada (1986) + O’Rourke, en 1992

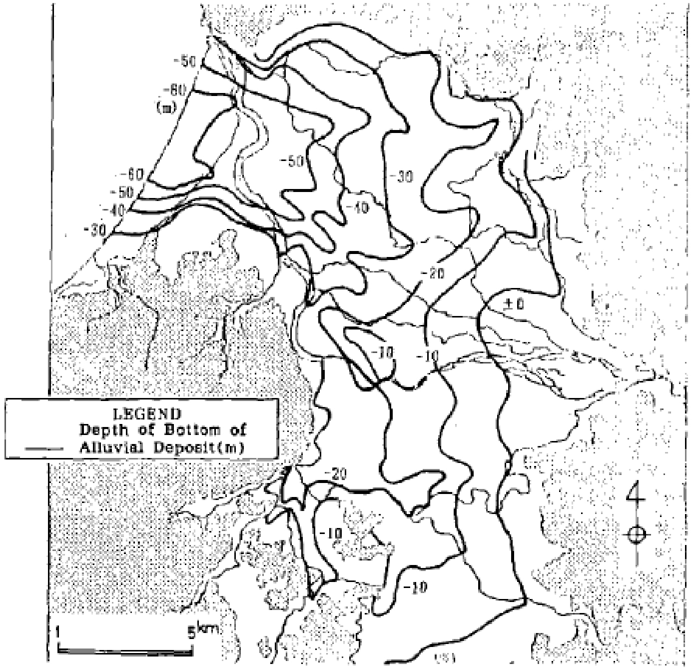

Figure 4. Depth of Alluvial Deposits under Fukui Plain

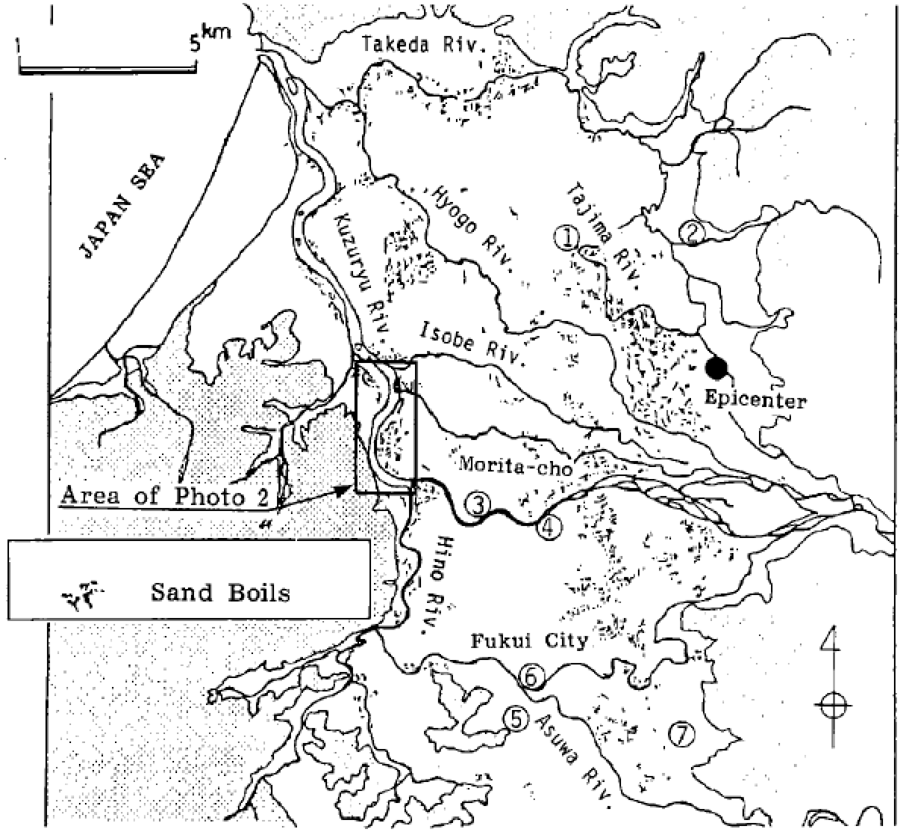

Figure 6. Sand Boils and Ground Fissures on Fukui Plain

1948 – Fukui - Japon

Liquéfaction en zone alluviale

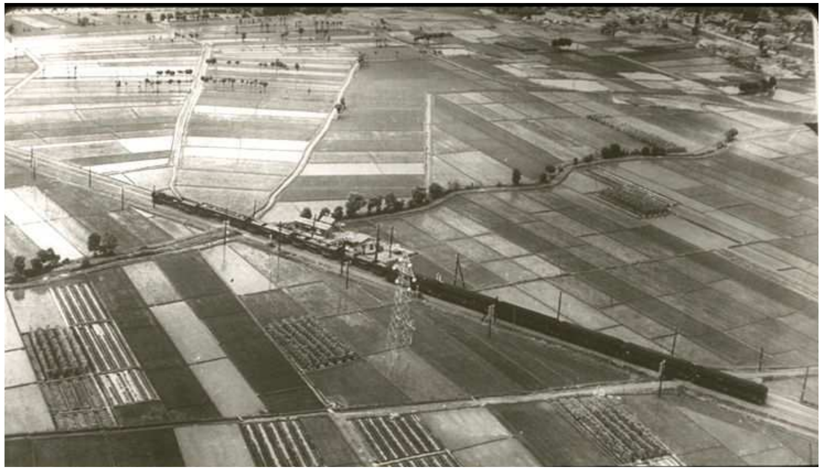

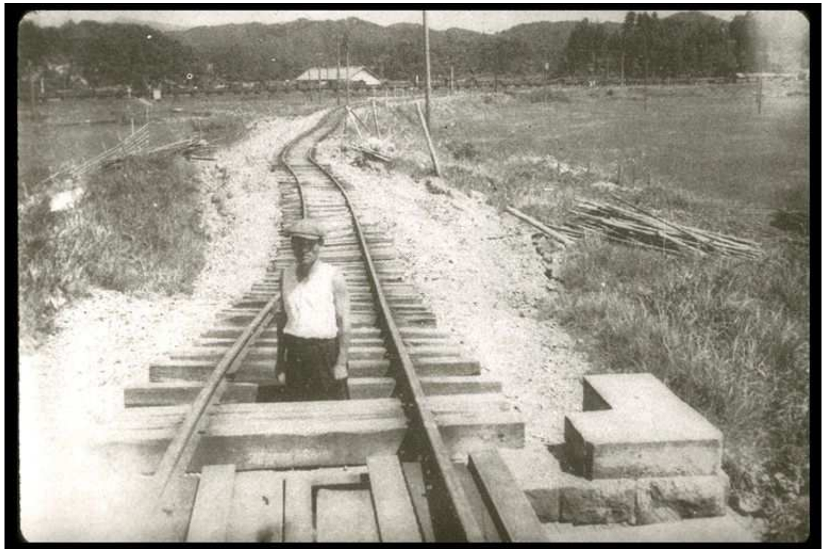

1948 – Fukui - Japon

Liquéfaction en zone alluviale

3 – Les années 1976-1988

+ Tangshan -1976

+ Guatemalaa - 1976

+ Japon : 1978 – Miyagui Ken Oki -Sendai

1983 – Nihonkai Chubu

+ 1980 : El Asnam (Algérie)

et Campania Lucania (Italie) : peu de liquéfaction

+ 1985 : Valparaiso : Quais

+ 1985 : Mexico : 1ère mission AFPS

pas de liquéfaction à Mexico City,seulement sur la côte

Ouest, près de l'épicentre.

A Lazaro Cardenas, usine sidérurgique bloquée pendant 6 mois,

à cause d'un problème de liquéfaction (?)– tapis roulant.

+ 1987 : Edgecumbe (NZ) : liquéfaction et prise en compte en NZ

+etc…

1976 – Tangshan

Liquéfaction en zones alluviale et marine récente

Overview Volume to the English Version

Report On

THE GREAT TANGSHAN EARTHQUAKE OF 1976

Chinese Version

Edited by: Liu Huixian

English Edition

Chairmen:
George W. Housner
Xie Lili

Editors:
George W. Housner
He Duxin

Published by

Earthquake Engineering Research Laboratory
California Institute of Technology
Pasadena, California

2002

1976 – Tangshan

Liquéfaction en zones alluviale et marine récente

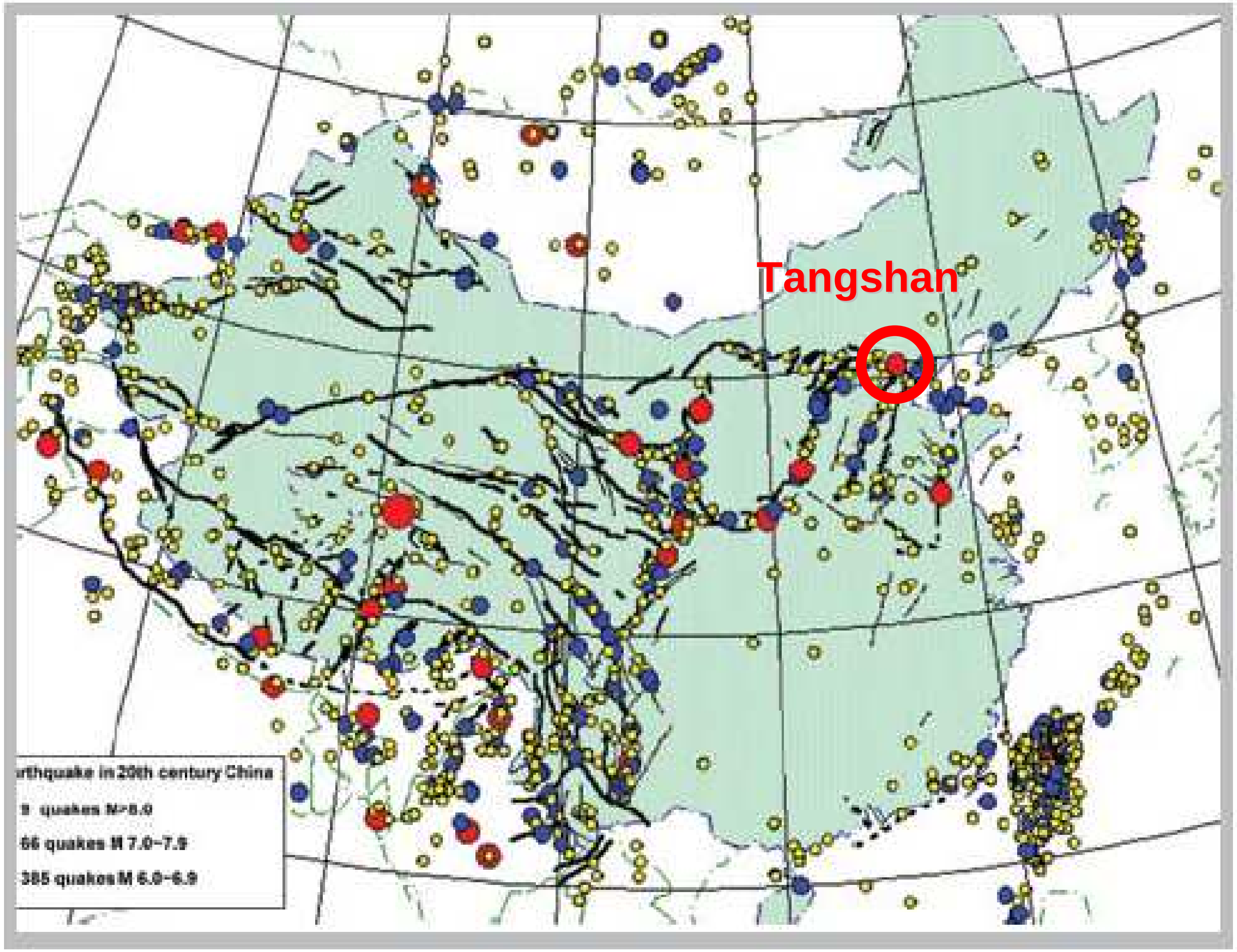

Distribution of earthquakes in China with magnitude 6 or above since 1900

1976 – Tangshan

Liquéfaction en zones alluviale et marine récente

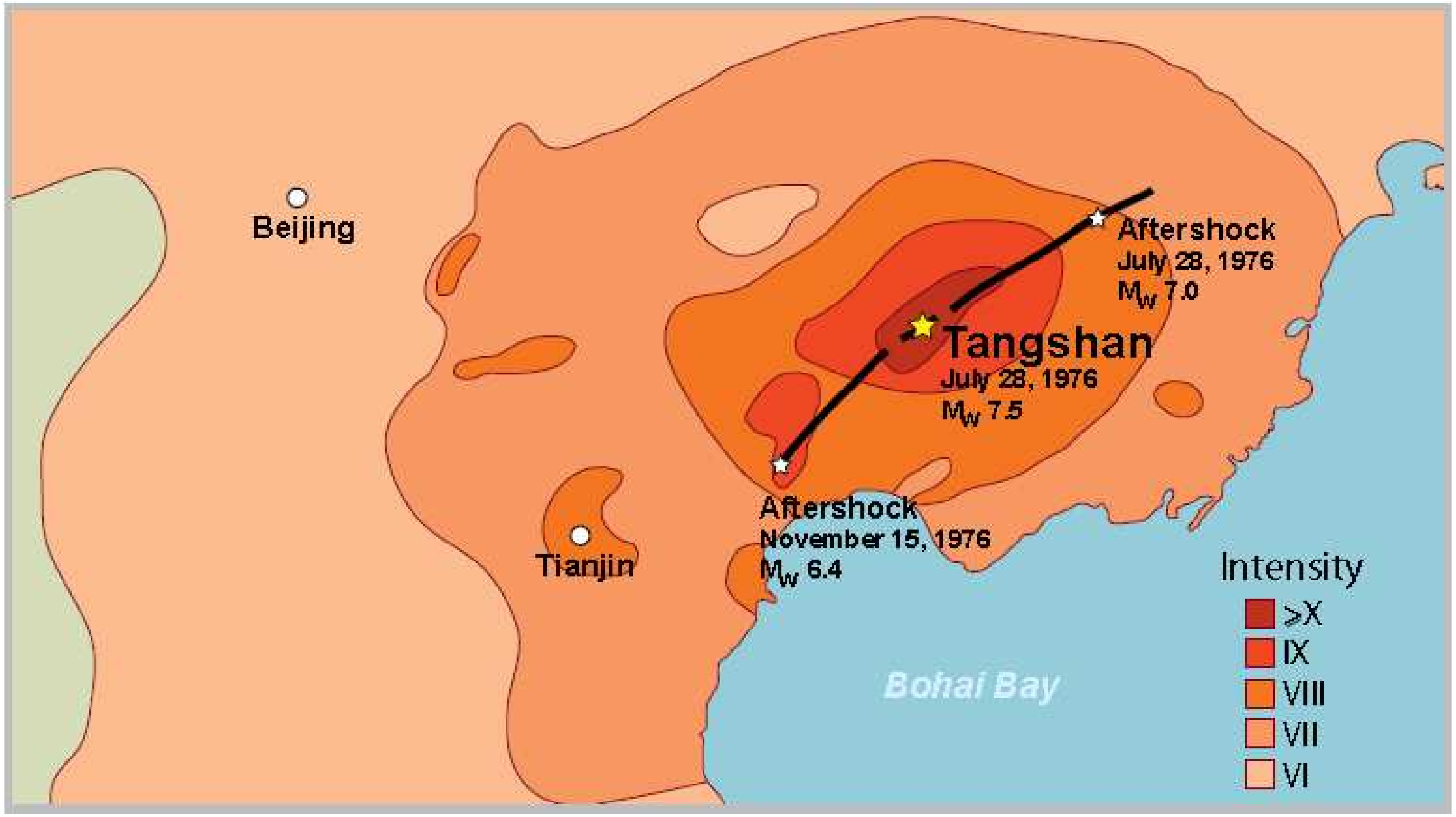

Intensity map of the 1976 Tangshan Earthquake, showing the Tangshan fault system and the epicenters of the July 28, 1976 Mw 7.5 event, the Mw 7.0 aftershock (northeast of Tangshan) and the Mw 6.4 aftershock (southwest of Tangshan)

1976 – Tangshan

Liquéfaction en zones alluviale et marine récente

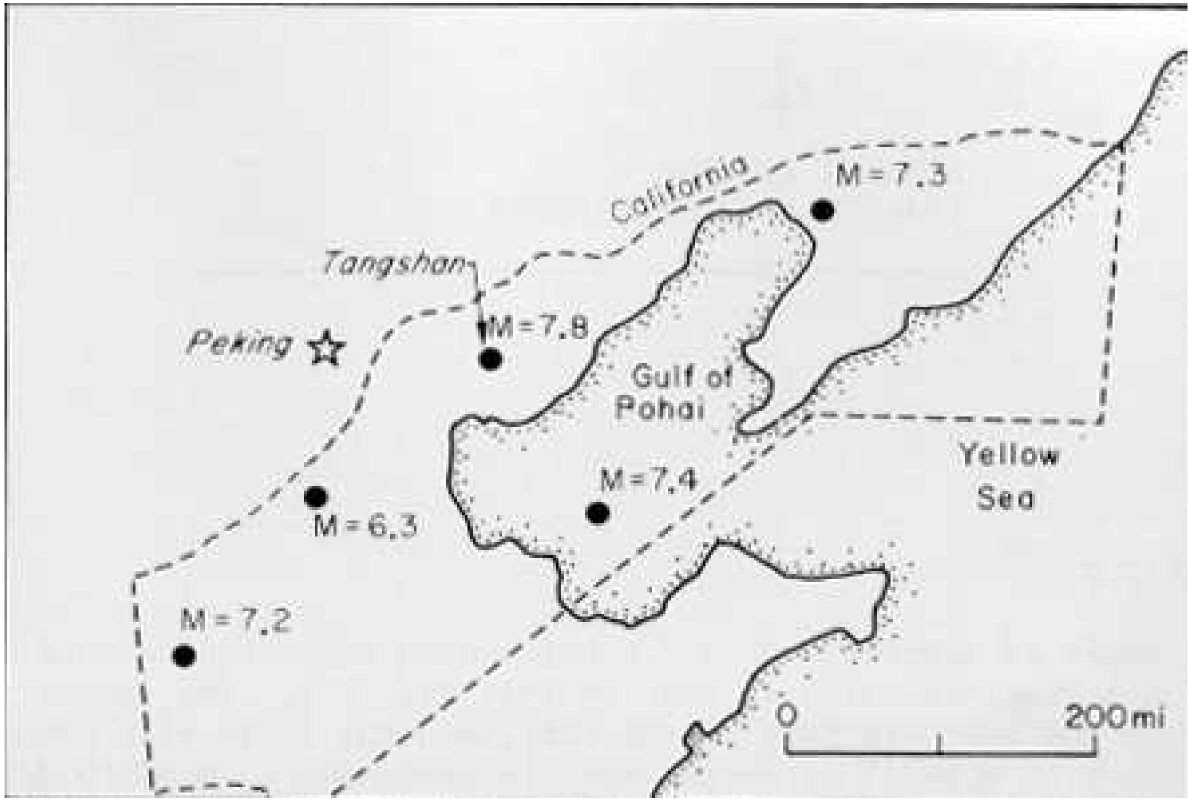

Figure 19. Epicenters of recent major earthquakes in Pohai region: Tangshan, July 28, 1976, M = 7.8; Haicheng, February 4, 1975, M = 7.3; Pohai, July 18, 1969, M = 7.4; Hojian, March 27, 1967, M = 6.3; Hsingtai, March 22, 1966, M = 7.2. The outline of the state of California is shown dotted, so it can be seen that within 15 years there were four earthquakes of magnitude greater than 7 in a region of approximately the same area as California.

2003 Pacific Conference on Earthquake Engineering

An assessment of the liquefaction susceptibility of Adapazari silt

R.B. Sancio, J. D. Bray & M.F. Riemer
University of California, Berkeley, USA.
T. Durgunoglu
Bogazici University, Istanbul, Turkey.

Based on the data from sites where liquefaction was and was not observed after earthquakes in China, Wang (1979) established that any clayey soil containing less than 15% to 20% particles by weight smaller than 5 mm and having a water content (wc) to liquid limit (LL) ratio greater than 0.9 is susceptible to liquefaction.

Based on this data, Seed and Idriss (1982) stated that clayey soils (i.e. plots above the A-line on the plasticity chart) could be susceptible to liquefaction only if all three of the following conditions are met:

(1) Percent less than 5 μm < 15%,

(2) LL < 35, and

(3) wc/LL > 0.9.

Due to its origin, this standard is known in the literature **as the "Chinese criteria."**

1976 – Tangshan

Liquéfaction en zones alluviale et marine récente

Koester (1992) noted that the determination of LL by means of the fall cone used in China produced values that are about 4 points higher than those values determined by means of the Casagrande percussion device. Hence, Koester recommended a slight reduction of the LL condition of the Chinese criteria before using it as a screening tool when the Casagrande method has been used. Similarly, Andrews and Martin (2000) reduced the LL condition for liquefaction susceptibility to < 32. Andrews and Martin then used 2mm as the limit between silt-size and clay-size particles, with < 10% clay-size particles being necessary for a silty or clayey soil to be liquefiable. Moreover, Andrews and Martin dropped the wc/LL ratio as a condition in their liquefaction susceptibilit y criteria of silty soils. After the 1989 Loma Prieta earthquake, Boulanger et al. (1998) noted that a deposit of clayey soil might have contributed to the surface deformations observed at the Moss Landing site. They concluded that indiscriminate use of the Chinese criteria as a substitute for detailed laboratory and insitu testing should be avoided. Similarly, Perlea (2000) recommends laboratory testing as the best way to evaluate the liquefaction susceptibility and post-cyclic undrained strength of cohesive soils. The location of a soil on the Casagrande plasticity chart and, or in combination with, the use of the "C« descriptor of the Unified Soil Classification System (USCS) have also been introduced as a tool to identify potentially liquefiable soils. Youd (1998) recommends the Chinese criteria as a generally conservative predictive tool. Additionally, he follows a series of assumptions to state that natural soil deposits that have a "C" descriptor (e.g. CH, CL, SC, and GC) are screened as nonliquefiable. Possibly liquefiable fine-grained soils should have LL < 35 and plot below the A-line or have PI < 7. Seed et al. (2001) indicate that soils that have LL < 30 and PI < 10 are liquefiable, and those with 30 < LL < 40 and 10 < PI < 12 fall into an "uncertain range". Undisturbed samples of soils that plot in that region of the plasticity chart should be obtained for laboratory testing. Polito (2001) used a wider range of the plasticity chart, and according to his criteria, soils with LL < 25 and PI < 7 are liquefiable. Soils that have 25 < LL < 35 and 7 < PI < 10 are potentially liquefiable, and finally soils with 35 < LL < 50 and 10 < PI < 15 are susceptible to cyclic mobility.

The current state-of-the-art and state-of-the-practice for liquefaction study is established in the summary report from the 1996 NCEER and 1998 NCEER/NSF workshops on evaluation of liquefaction resistance of soils (Youd et al., 2001). **Therein, the use of the Chinese criteria is recommended to confirm the liquefaction susceptibility of silts and clays.**

5 **CONCLUSIONS**

Based on a large number of cyclic triaxial tests performed on "undisturbed" specimens of Adapazari silt and silty clay of low penetration resistance [$(N1)60 < 10$], the following conclusions are drawn:

1. The Chinese criteria is not effective for the evaluation of liquefaction susceptibility of fine grained soils with PI < 12, due primarily to the ineffectiveness of the condition on the amount of particles smaller the 5µm. Additionally, this testing program has shown that soils with 12 < PI < 20, which generally have LL > 35, can generate significant strains in a small number of cycles when a high CSR is applied.
2. Plasticity Index in combination with wc/LL appears to be a good indicator of soil liquefaction susceptibility. Fine grained soils from Adapazari with PI < 12 and wc/LL > 0.8 are susceptible to liquefaction, and soils of 12 < PI < 20 and wc/LL > 0.8 should be tested in the laboratory to assess their liquefaction susceptibility.
3. A limited number of tests that were performed on specimens with PI > 20 with wc/LL < 0.8 did not generate significant cyclic strains after a large number of cycles had been applied at initial confining stresses < 50 kPa.
4. The fact that ground failure in Adapazari was primarily observed adjacent to buildings may be attributed to, among other factors, the detrimental effect of an increase in confining stress on the cyclic strength when represented in terms of the cyclic stress ratio.
5. This testing program has shown that limiting $K\sigma < 1.0$ in design as suggested by Youd et al. (2001) may be overly conservative at low effective confining stresses.

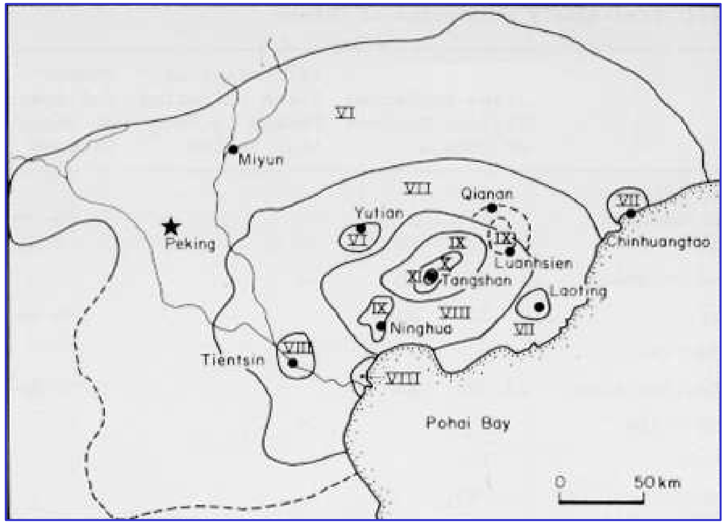

Figure 20. Intensity map of the 1976 Tangshan earthquake. The dotted lines represent a large aftershock. The Chinese intensity scale is similar to the Modified Mercalli intensity scale, but construction in China is quite different from construction in the United States, so that direct comparisons cannot be made.

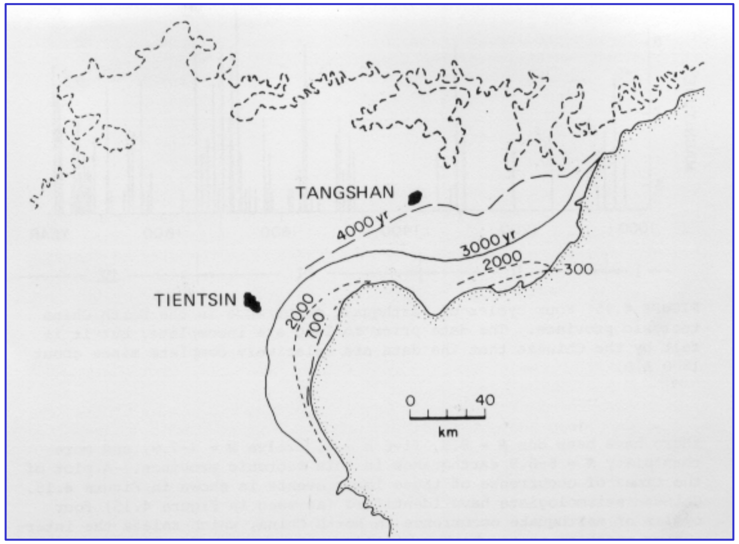

Figure 32. Map showing how the shoreline has advanced over the past 4,000 years. The shoreline 4,000 years ago passed just south of Tangshan City site; the map shows where the shoreline was 3,000 years ago, and the present location. This makes clear why there were so many soft soils south of Tangshan

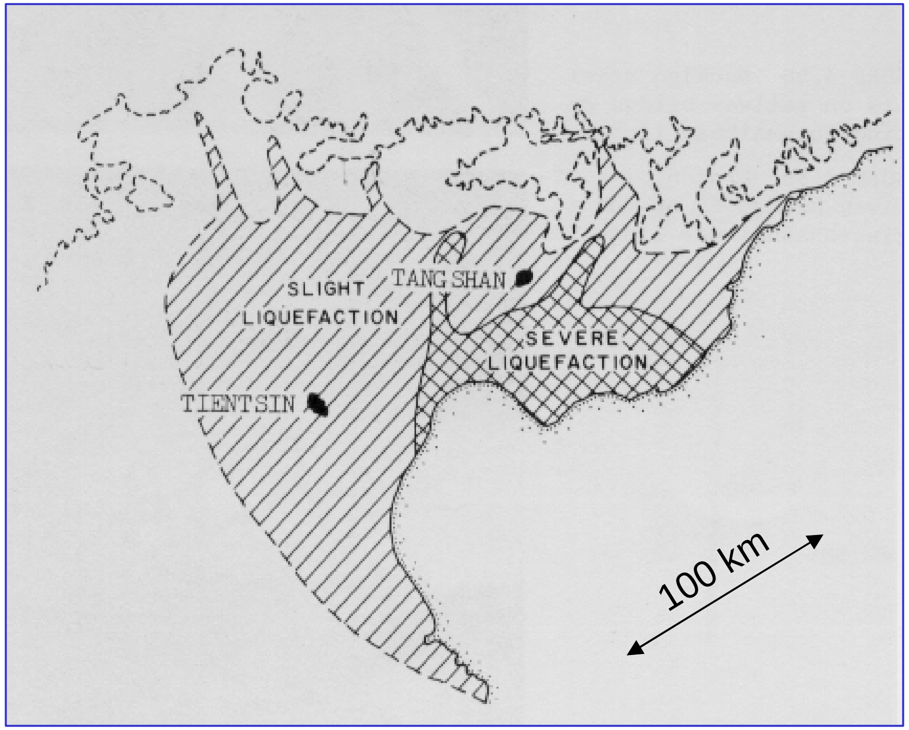

Figure 78. Map of Tangshan-Tientsin region showing areas of liquefaction

1976 – Tangshan

Liquéfaction en zones alluviale et marine récente

Figure 23. Damage to road near Loting Hsien. Slumping, lurching and settlement of soft soils caused extensive damage to highways in the Tangshan region.

1983 – Nihonkai Chubu

Liquéfaction en zone alluviale - Noshiro

Nihonkai Chubu – 26 mai 1983

M = 7.7 amax = 0.20 g à Akita

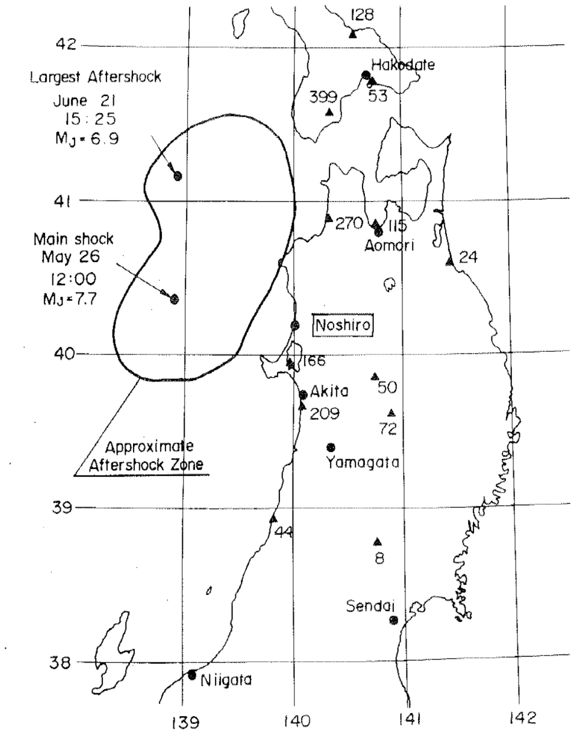

▲ Maximum Horizontal Acceleration in gal Observed by Strong Motion Seismograph (SMAC Type)

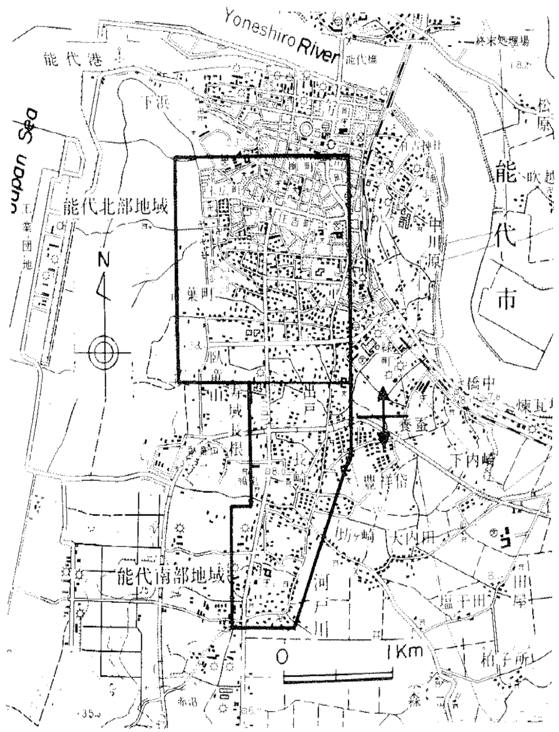

Fig. 2-2 Measured area of permanent ground displacement in Noshiro City

Evaluation des déplacements horizontaux et des formes superficielles

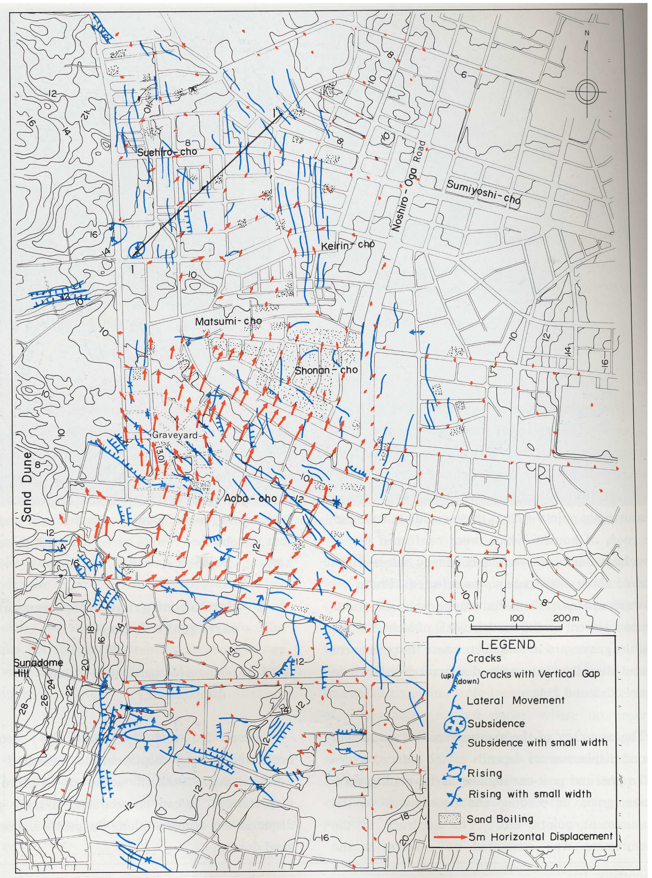

Fig. 2-3 Permanent horizontal ground displacements in the northern part of Noshiro City

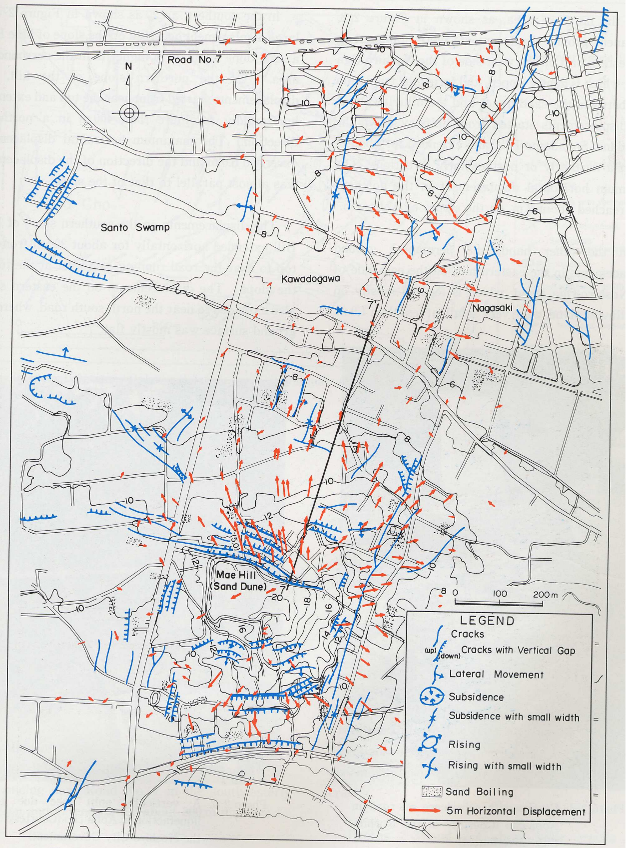

Fig. 2-4 Permanent horizontal ground displacements in the southern part of Noshiro City

1983 – Nihonkai Chubu

Liquéfaction en zone alluviale + Quais - Noshiro

Liquéfaction – Retours d'expériences

3 - Les années 1976-1988

+ Toujours nombreuses recherches, en particulier à Berkeley, Caltech, MIT, au Japon, etc.., permettant d'améliorer l'utilisation de la « méthode simplifiée » de Seed-Idriss . Mais on en reste encore au SPT, pour les application pratiques courantes, sauf Nouvelle-Zélande et France : CPT et U et autres + US-Stokoe pour Vs.

+ Prise en compte des critères chinois.

+ Monographie de Seed-Idriss, publiée par EERI en 1982

+ Workshop NSF, organisé par Whitman en 1985 pour obtenir consensus sur les méthodes d'évaluation.

+ Modélisation dynamique non linéaire 2D et 3D : DYNAFLOW (Prévost), GEFDYN (Aubry, Modaressi), ………

+ Indice de potentialité de liquéfaction : LPI – Iwazaki et al, puis utilisation dans des microzonages sismiques : en particulier, Holzer pour les US

Liquéfaction – Retours d'expériences

4 – Les années 1989-1998

+ Loma Prieta -1989, mission AFPS

+ Northridge – 1994, mission AFPS

+ Japon : 1995 – Kobe ou Hyogo Ken Nanbu, mission AFPS

+ Autres séismes marquants : Manjil (Iran) -1990 (AFPS)

Luzon (Philippines) -1991, Limon (Costa Rica) – 1991, Erzincan (Turquie) -1992 (AFPS) et Ceyhan-Adana (Turquie) -1996 (AFPS)

+ Recherches étendues après les séismes américains et le séisme de Kobe, en particulier : Projets mondiaux comme VELACS, etc…Quelle modélisation en dynamique non linéaire ?

+etc…

Loma Prieta – 17 octobre 1989

M = 6.9 amax → 0.33 g (SF) et 0.6 g à l'épicentre

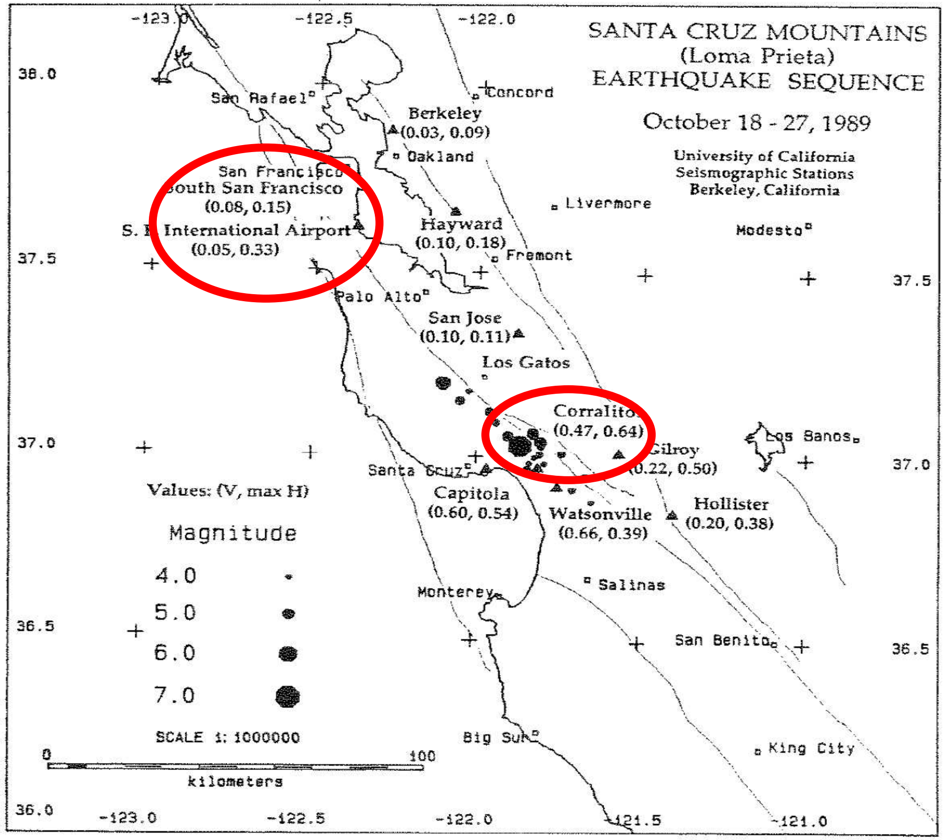

Fig. 1.1: Map of area of highest intensity, showing epicenters of main shock and largest aftershocks. Peak vertical and horizontal accelerations are shown at some sites (most, courtesy A. Shakal, SMIP).

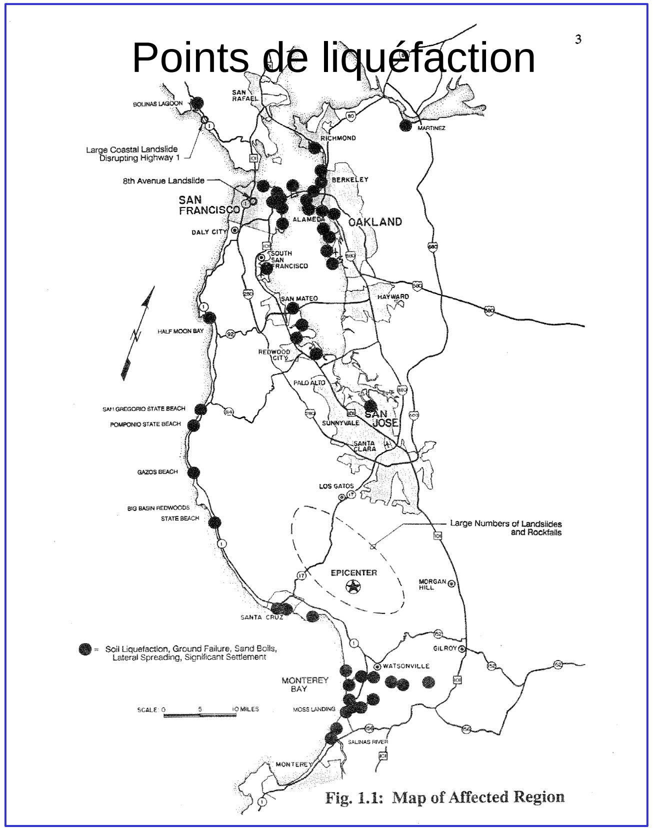

Fig. 1.1: Map of Affected Region

1989 – Loma Prieta

Liquéfaction en zones alluviale et marine + Remblais

1989 – Loma Prieta

Liquéfaction en zones alluviale et marine + Remblais

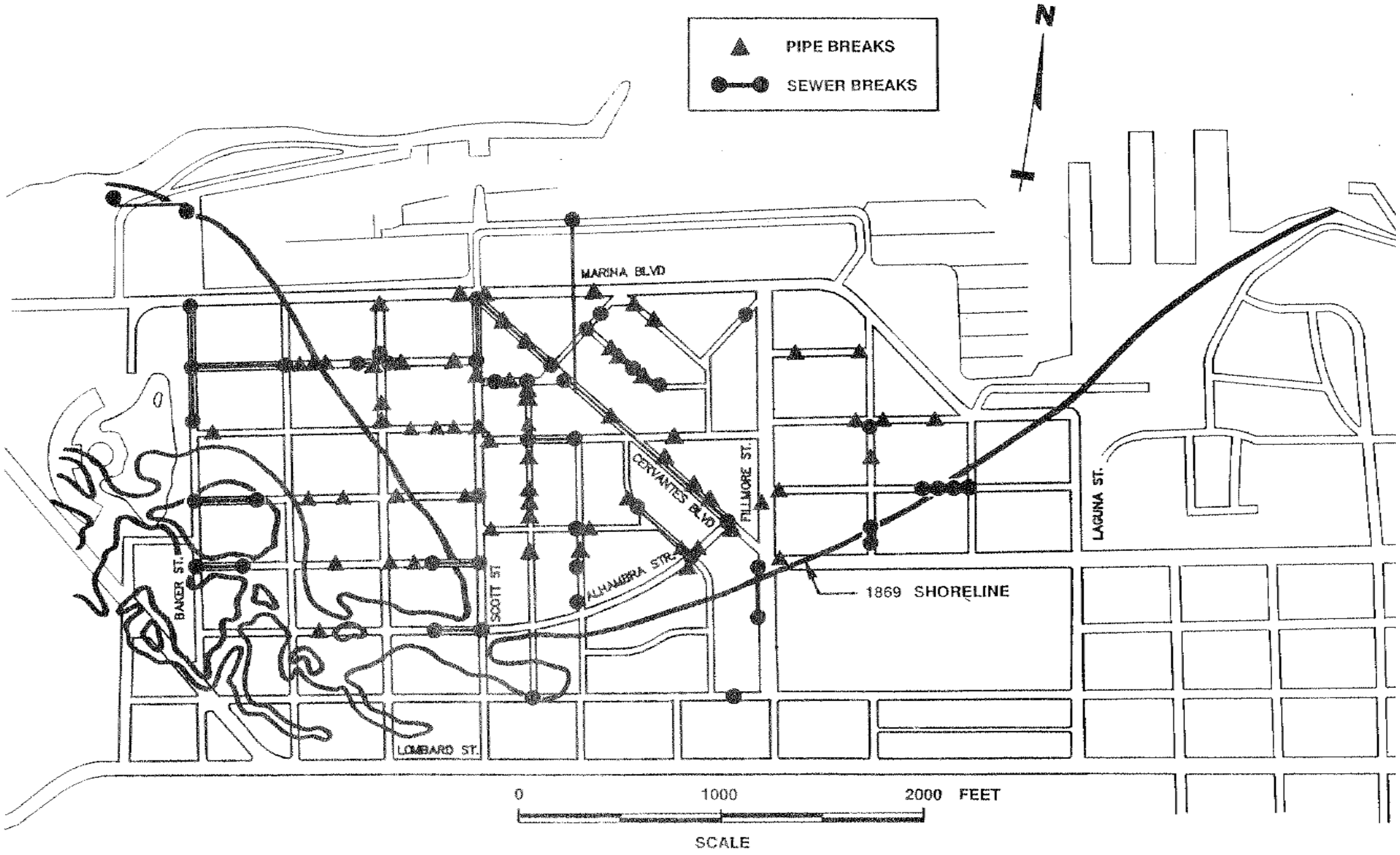

Fig. 3.11 Locations of Major Water Pipe and Sewer Breaks; Marina District, San Francisco

1989 – Loma Prieta

Liquéfaction en zones alluviale et marine + Remblais

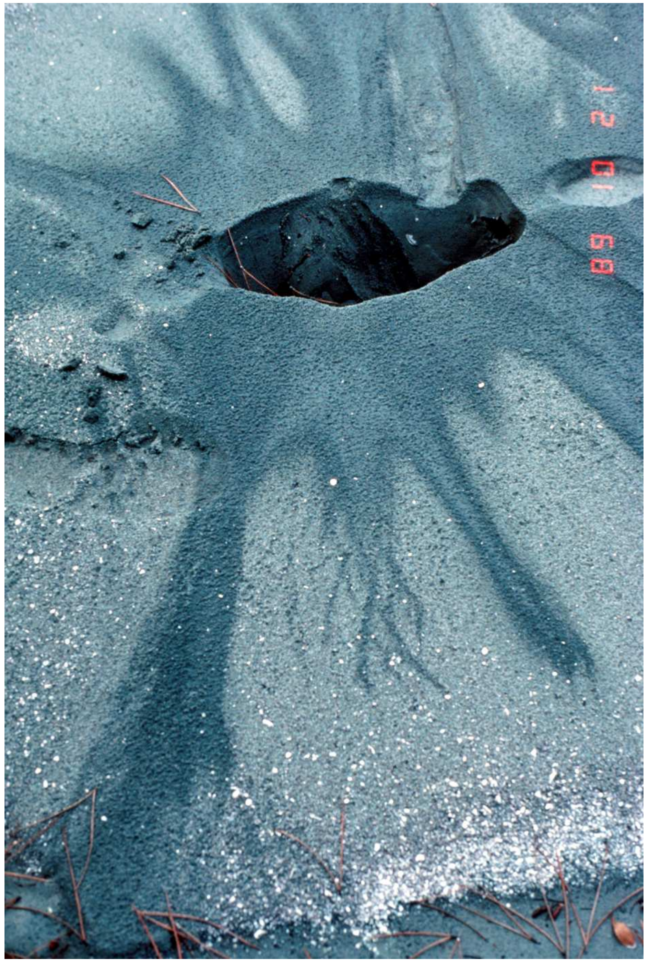

1989 – Loma Prieta

Liquéfaction en zones alluviale et marine + Remblais

1989 – Loma Prieta

Liquéfaction en zones alluviale et marine + Remblais

Kobe - Hyogo Ken Nanbu 17 janvier 1995

M = 6.8 amax jusqu'0.8 g

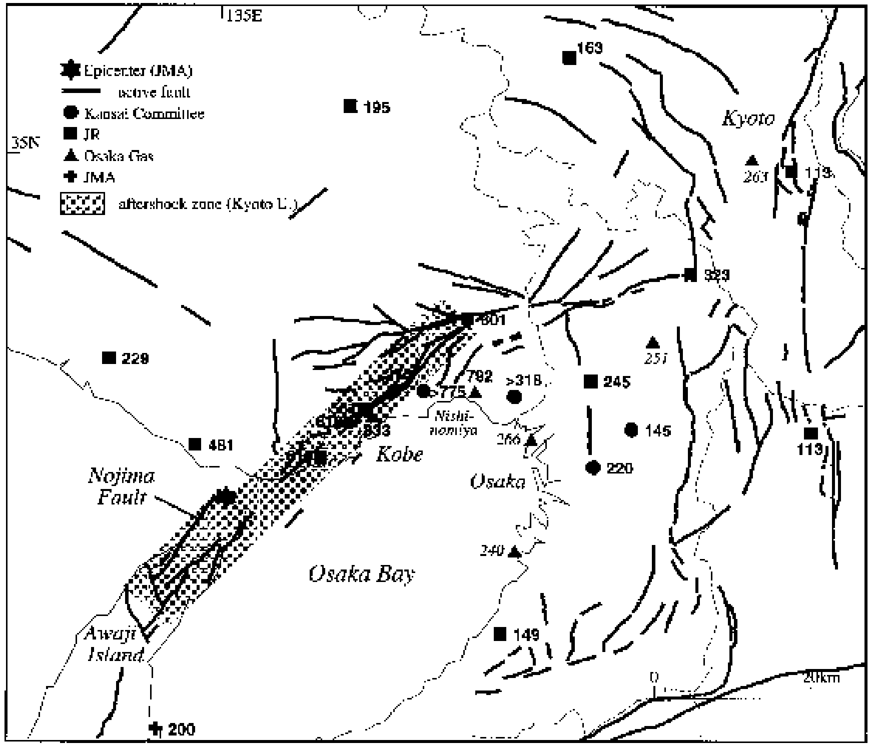

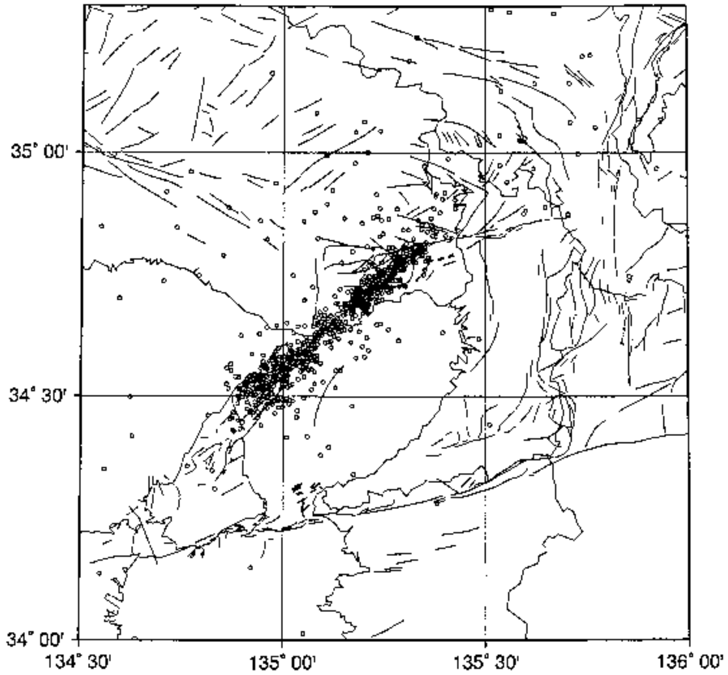

1995 – Kobe Hyogo Ken Nanbu

Liquéfaction en zone marine + Remblais

1995 – Kobe Hyogo Ken Nanbu

Liquéfaction en zone marine + Remblais

1995 – Kobe Hyogo Ken Nanbu

Liquéfaction en zone marine + Remblais

1995 – Kobe Hyogo Ken Nanbu

Liquéfaction en zone marine + Remblais

1995 – Kobe Hyogo Ken Nanbu

Liquéfaction en zone marine + Remblais

1995 Kobe Earthquake –
Example of damage to port facilities
Source – Kobe Geotechnical Collection,
Earthquake Engineering Research Center,
University of California, Berkeley

Example of main sewage treatment conduit rupture in the 1995 Kobe Earthquake
Source – Kobe Geotechnical Collection, Earthquake Engineering Research Center, Univ. of California, Berkeley

1995 – Kobe Hyogo Ken Nanbu

Liquéfaction en zone marine + Remblais

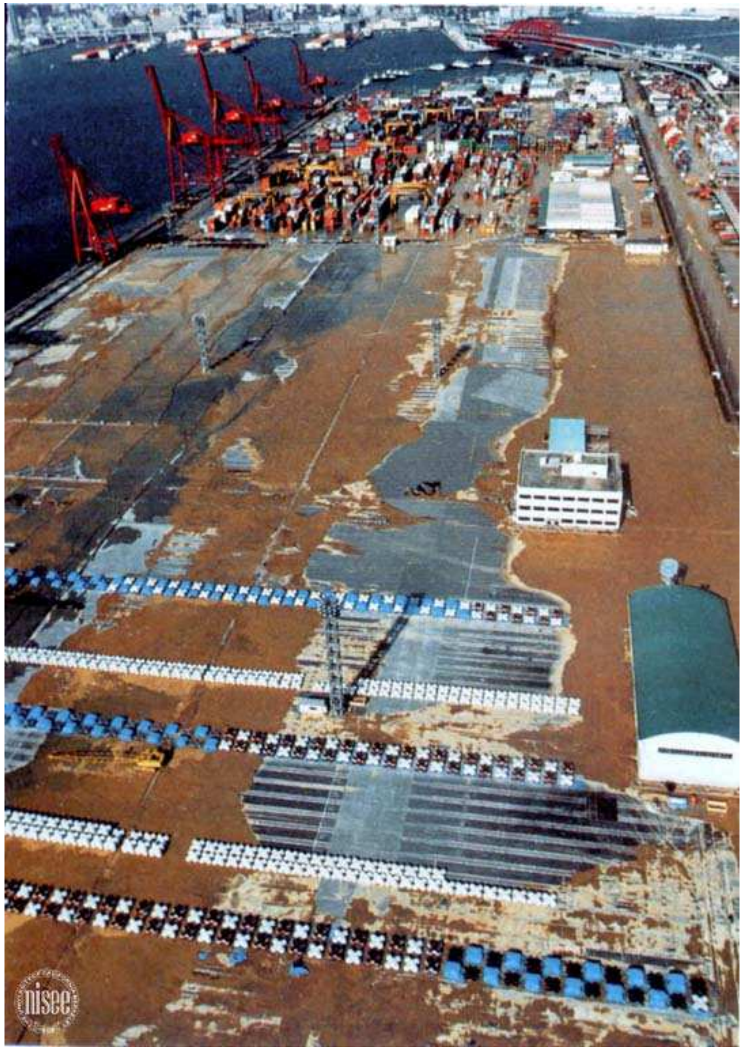

1995 – Kobe Hyogo Ken Nanbu

Liquéfaction en zone marine + Remblais

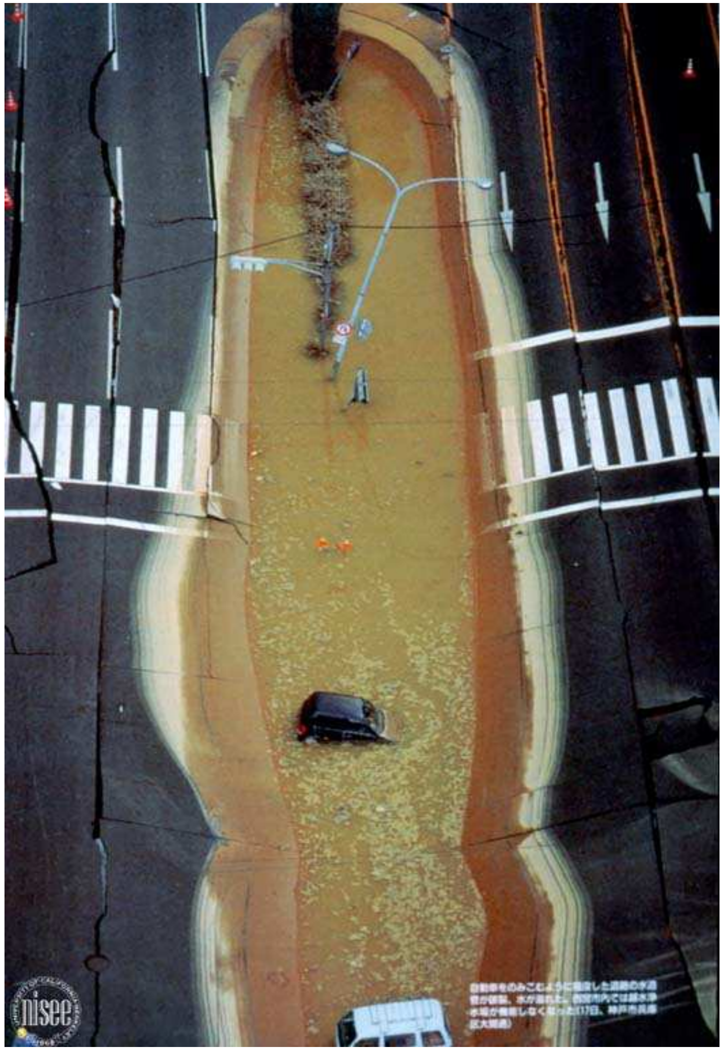

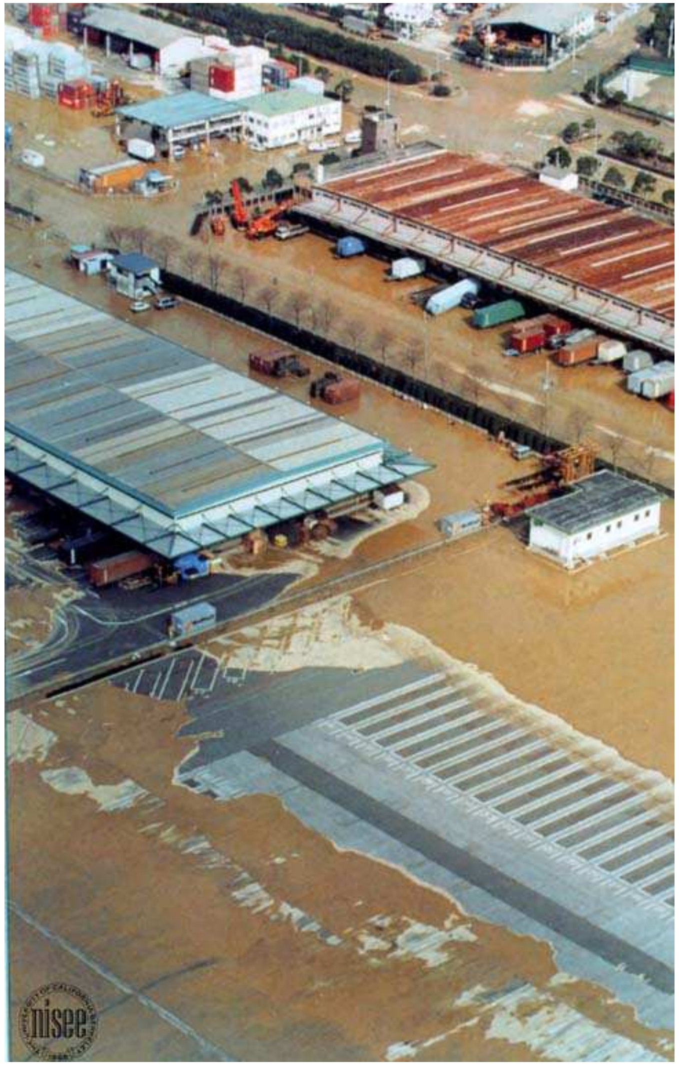

Ceyhan – Adana (Turquie)

M = 6.2 amax > 0.25 g

1998 – Ceyhan – Adana (Turquie)

Liquéfaction en zones alluviale

Particularité du mouvement sismique à Ceyhan-Adana

(Mehmet Celeby - USGS)

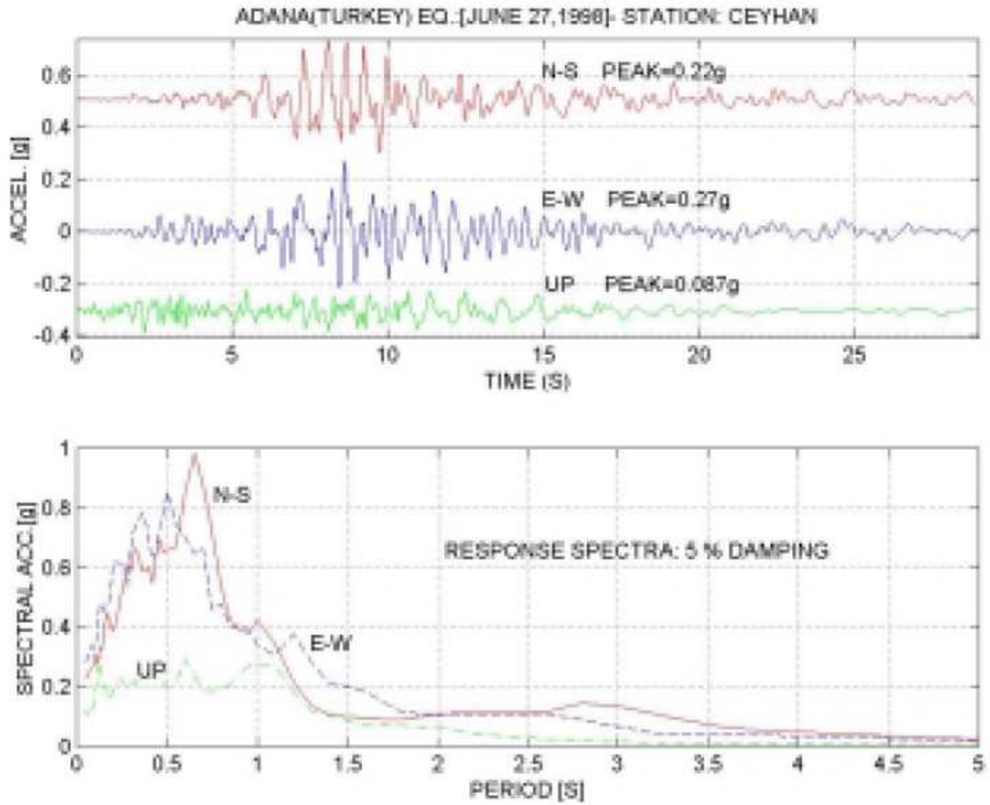

Figure 2. Strong-motion records from the Ceyhan Station (on the ground floor of a three-story building) and corresponding response spectra.

1998 – Ceyhan – Adana (Turquie)

Liquéfaction en zones alluviale

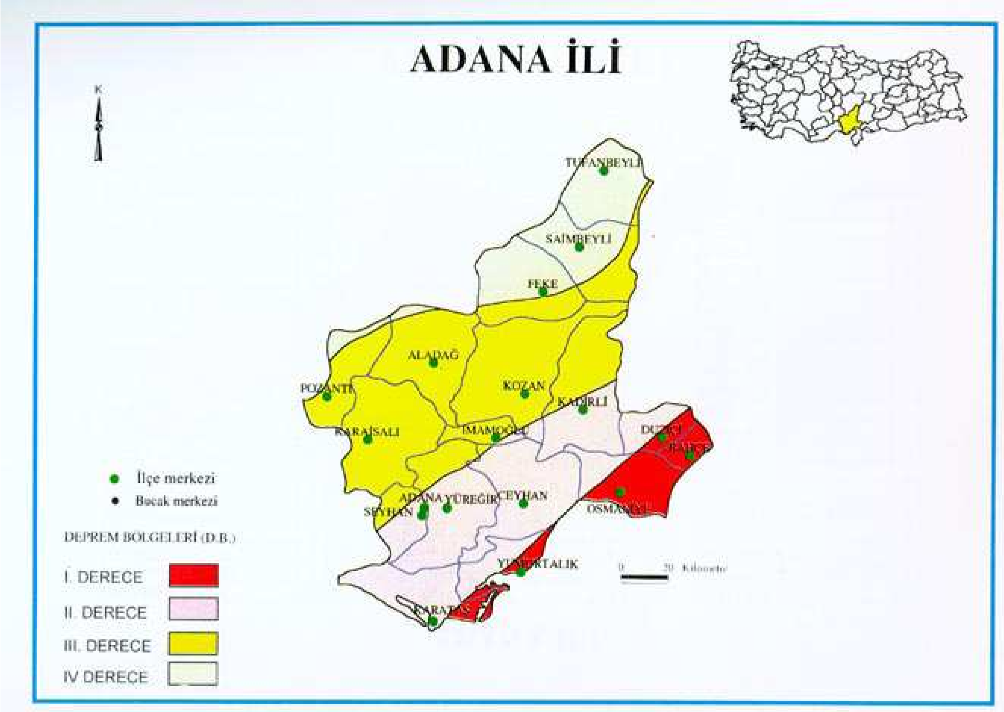

Fig. 39 Seismic Zones in the Adana-Ceyhan region showing Adana and Ceyhan in seismic zone II (Gencoglu 1996)

Liquéfaction – Retours d'expériences

4 – Les années 1989-1998

+ Loma Prieta -1989, mission AFPS

+ Northridge – 1994, mission AFPS

+ Japon : 1995 – Kobe ou Hyogo Ken Nanbu, mission AFPS

+ Ceyhan-Adana – Turquie, mission AFPS

+ Workshop spécial sur les méthodes d'évaluation du potentiel de liquéfaction en 1996 , organisé sous l'égide du NCEER, par Youd et Idriss – une vingtaine de spécialistes, puis par le NCEER/NSF en 1998.

Balayage de toutes les méthodes, avec SPT, CPT, Vs, BPT, y compris méthodes probabilistes et basées sur la prise en compte de l'énergie entrante (Demande).

+ Workshops US-Japan : 1996

+ Nombreuses recherches, dont VELACS et Modélisations

+ Début de création de méga-banques de données

+ etc…

Liquéfaction – Retours d'expériences

5 – Les années 1999-2009

+ Kocaeli (Turquie) -1999, mission AFPS

+ Chi Chi (Taiwan) - 1999, mission AFPS

+ Bhuj (Inde) - 2001, mission AFPS

+ Japon : Niigata Chuetsu – 2004,

Niigata-Kashiwazaki-Karima – 2007, mission AFPS

+ Boumerdes – 2003 (AFPS), Bam -2003 (AFPS), Sumatra – 2004, Pakistan – 2005, Indonésie, dont plusieurs à Java et Sumatra, les derniers près de Padang en 2009,

Perou – 2007, Sichuan – Wenchuan -2008

+ Grande banque de données avec les 2 premiers séismes

+ Workshops US-Japon et US-Taiwan

+ Nombreuses recherches, surtout pour préciser les paramètres de la méthode dite simplifiée et en modélisation

+ etc…

1999 – Kocaeli Izmit, Gölcuk, Adapazari, le 17 aout 1999

M = 7.4   amax ➔0.40 g

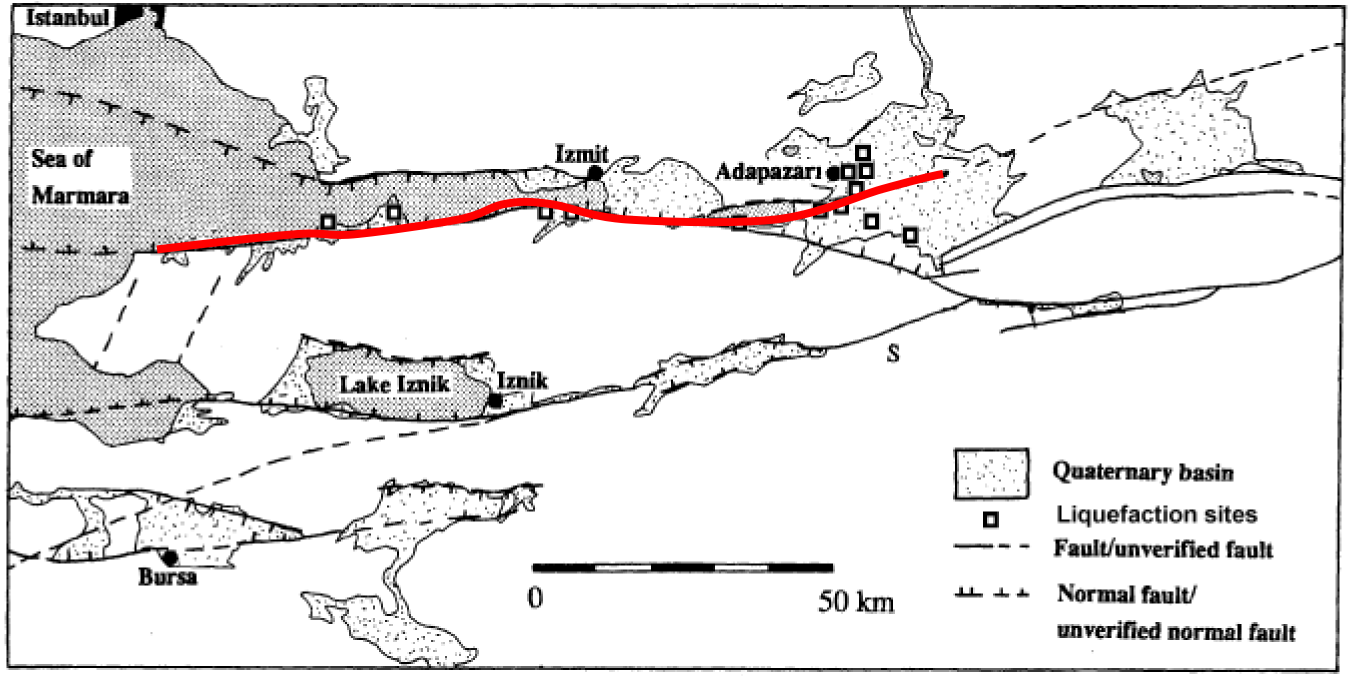

Figure 12.1 Distribution of liquefaction sites observed in this earthquake

Liquéfaction en zones alluviale et marine + Remblais

1999 – Kocaeli Izmit, Gölcuk, Adapazari

Liquéfaction en zones alluviale et marine + Remblais

1999 – Kocaeli Izmit, Gölcuk, Adapazari

Liquéfaction en zones alluviale et marine + Remblais

1999 – Kocaeli Izmit, Gölcuk, Adapazari

Liquéfaction en zones alluviale et marine + Remblais

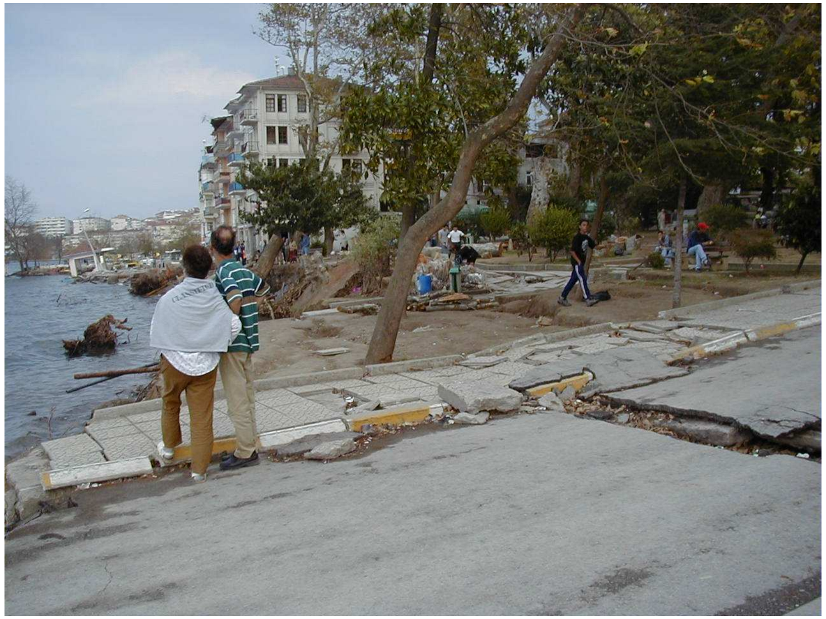

Figure 12.2 Sand volcano observed on Aug. 18, 1999 in Erenler (Adapazar)

1999 – Kocaeli Izmit, Gölcuk, Adapazari

Liquéfaction en zones alluviale et marine + Remblais

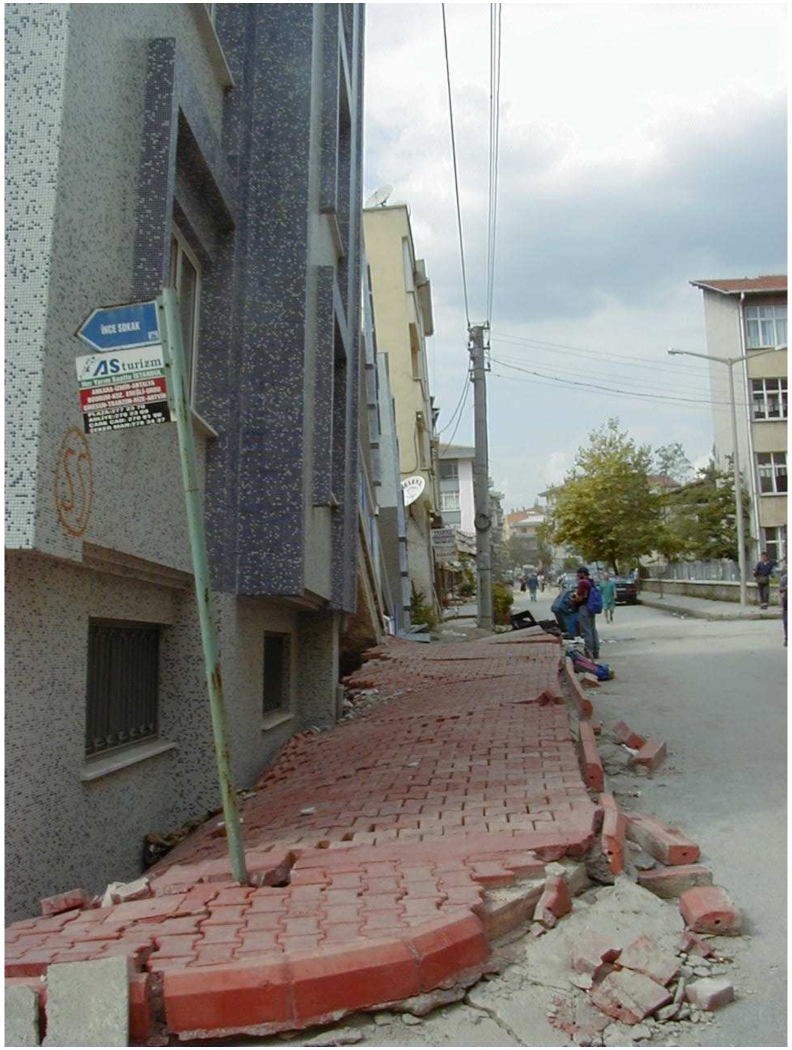

1999 – Kocaeli Izmit, Gölcuk, Adapazari

Liquéfaction en zones alluviale et marine + Remblais

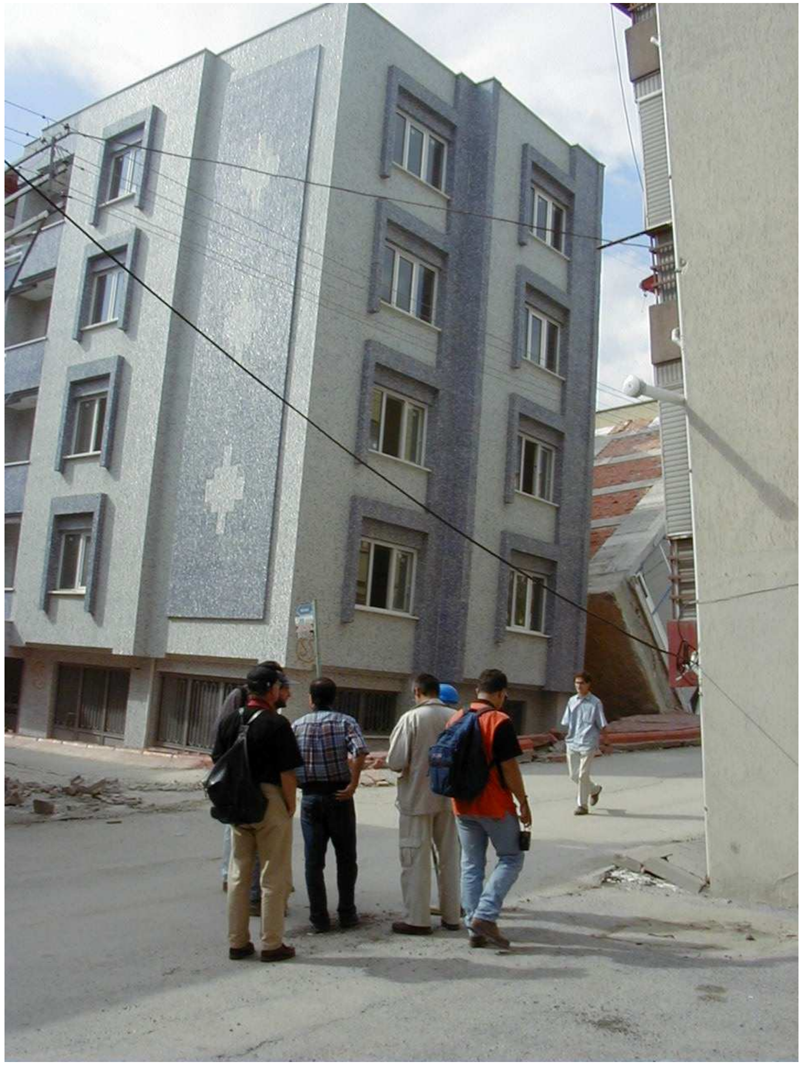

Chi Chi – Taiwan, le 20 septembre 1999

Mw= 7.6 amax jusqu'à 0.8 g

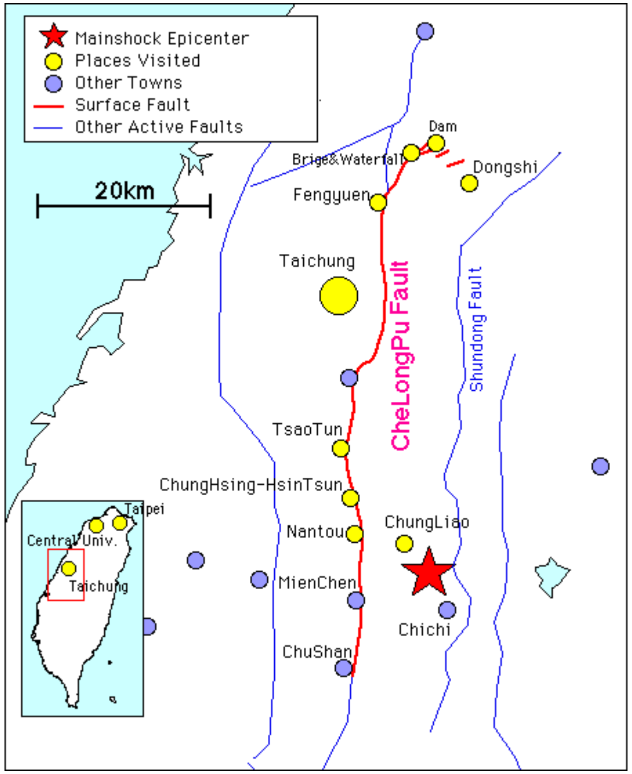

Glissement horizontal d ’un canal situé près du palais du gouvernement

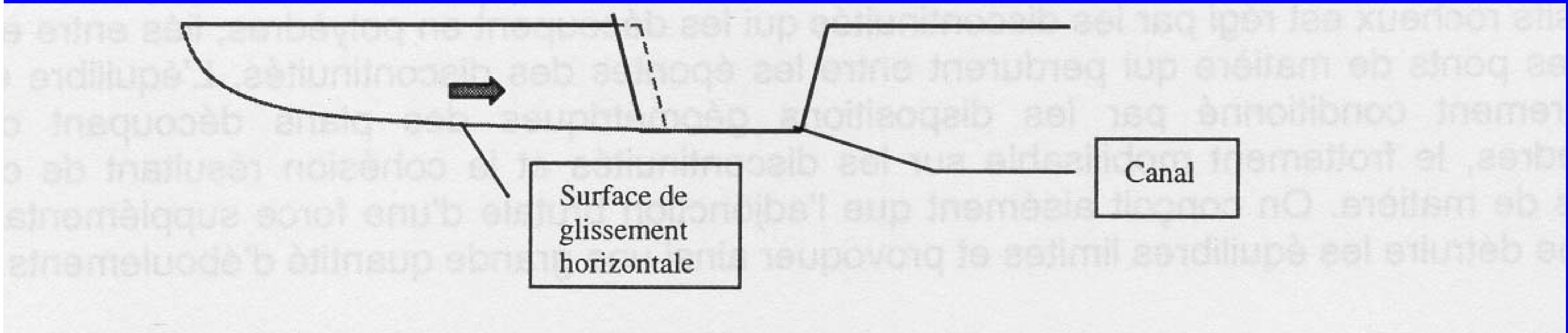

Lateral spread

J.P. Méneroud – C. Boutin AFPS

Glissement horizontale (lateral spread)

Liquéfaction

Trace de liquéfaction en surface

Sinkhole initially created by liquefaction but expanded significantly due to washout of sand between caissons.

Liquefaction at inward side of levee and at base of power line tower foundation shown in background.

Settlement failure due to liquefaction.

Nantou City

- Population 94k
- < 5 km from fault
- a_{max} = 0.38 g (TCU076)

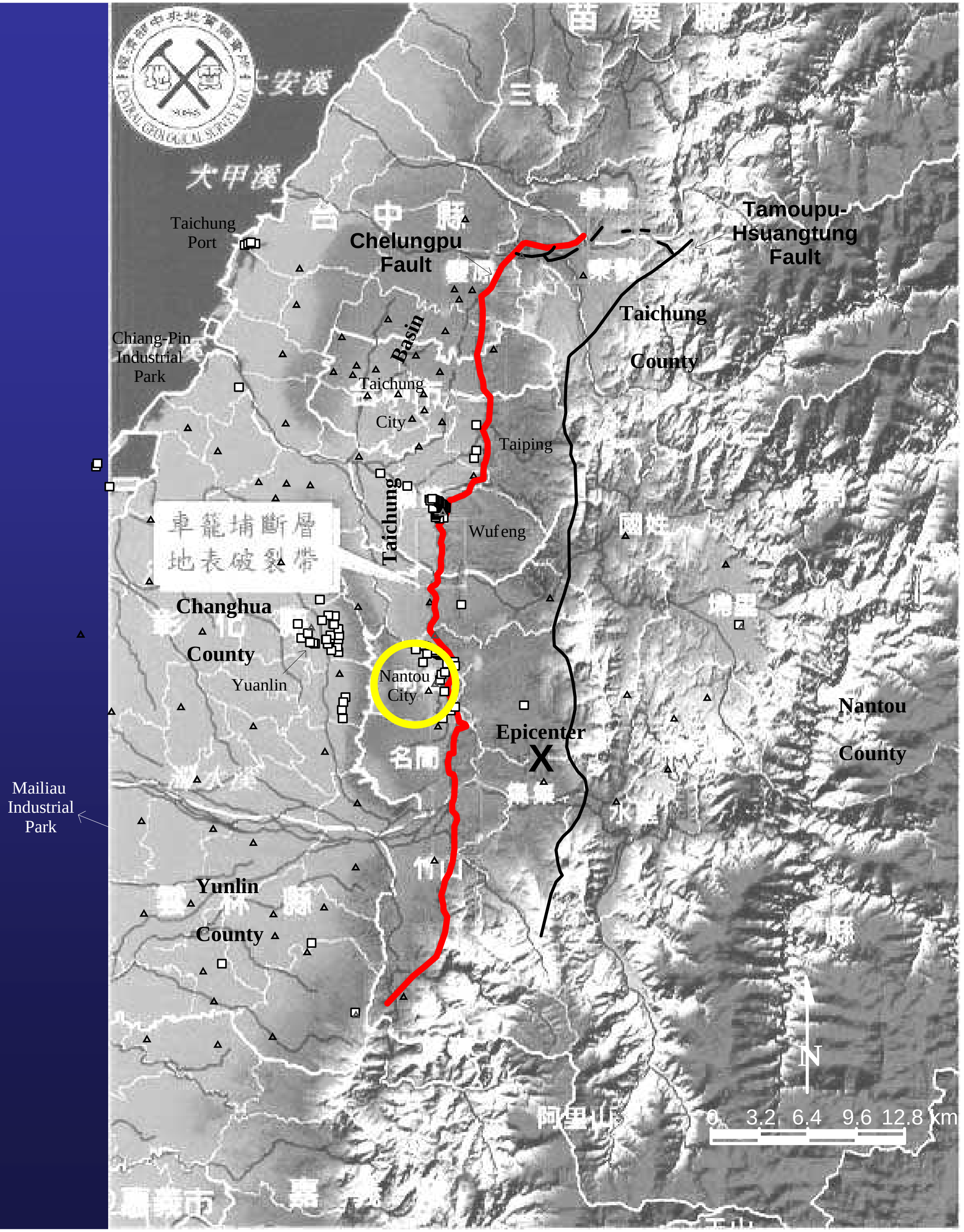

- Lateral spreading along river
- Subsidence/tilting of buildings

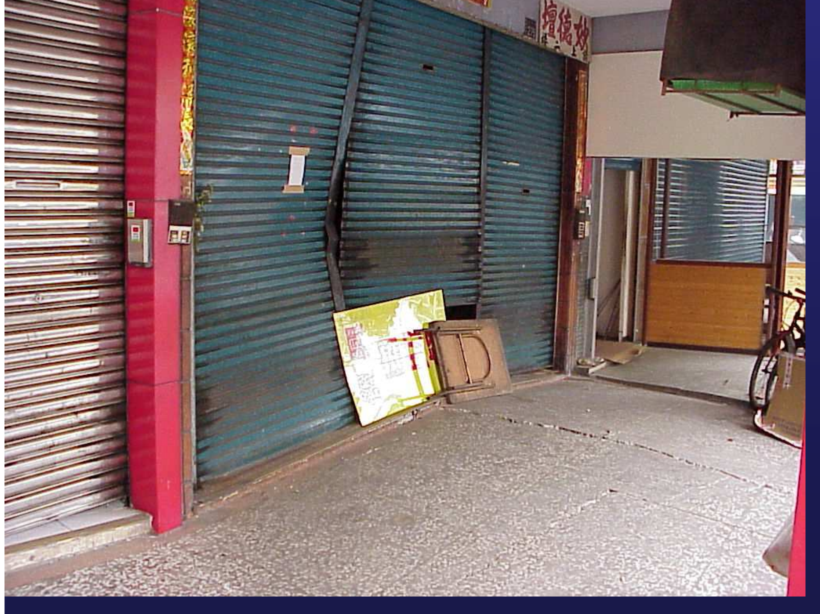

Wufeng Village

- Population 61k
- overlies fault
- $a_{max} = 0.67$ g (TCU065)

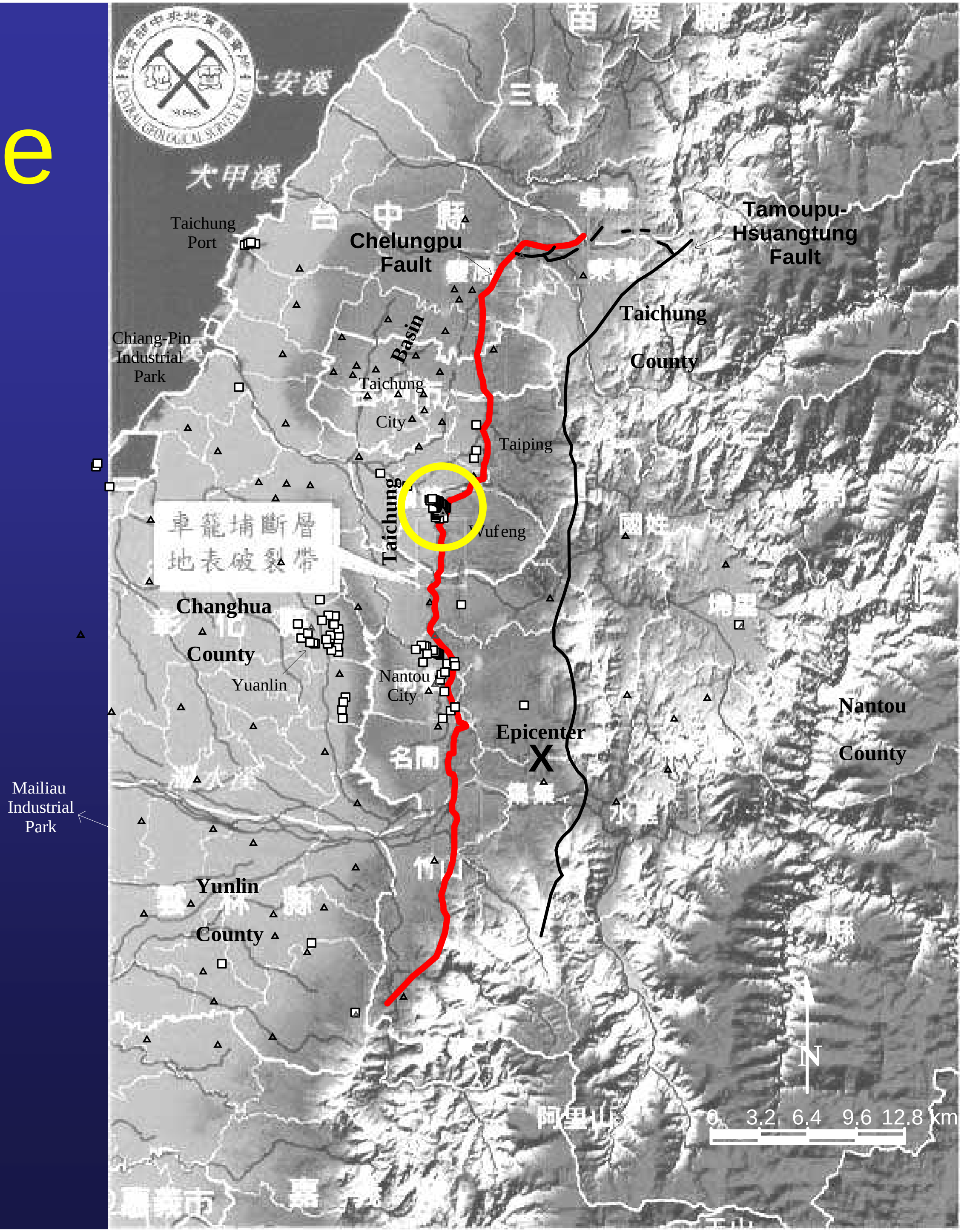


Tsao-Hu River
W-N-B2
Shih-The (Route 127) Road
W-N-B3
W-N-B1
W-N-C9
W-N-B5
W-N-B13
W-N-B11
W-N-C16
W-P-D
Ground Surface Rupture
Dry Creek River
W-N-B7
W-P-E
Road
Road
TCU 065
W-N-B8
W-P-A
W-N-B9
W-P-B
W-P-C
Dove Nest Creek
N
TCU 065 Strong Motion Accelerograph
Settled, Tilted Buildings
Lateral Spread
Sediment Boils
Surface Fault Rupture
NCREE Investigation Site
PEER Investigation Site

2001 – Bhuj - Inde

Liquéfaction en zones alluviales

Magnitude : 7.7 Ms
Profondeur : 23 km
(USGS - 31/01/2001)

⇨ **Forte probabilité de propagation de la rupture jusqu'en surface**

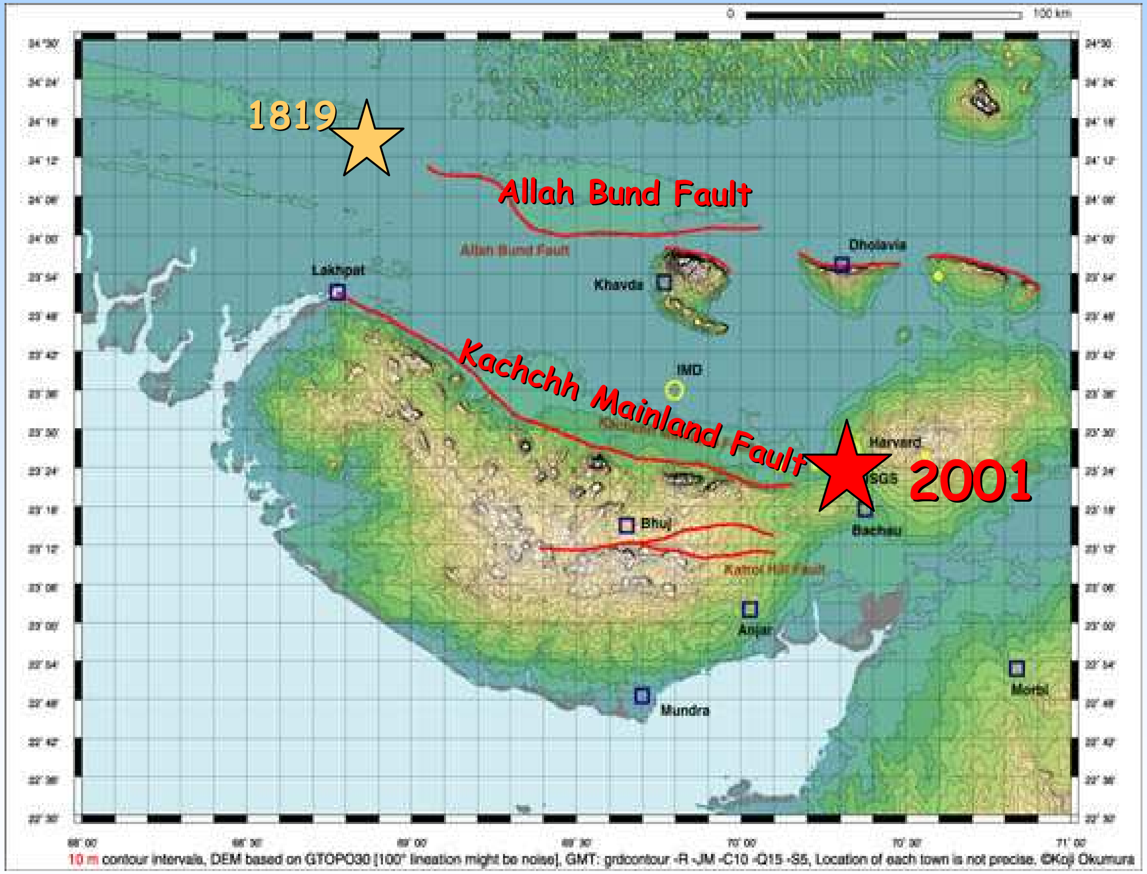

O. Sedan, Jean-Louis Durville, Claude Boutin

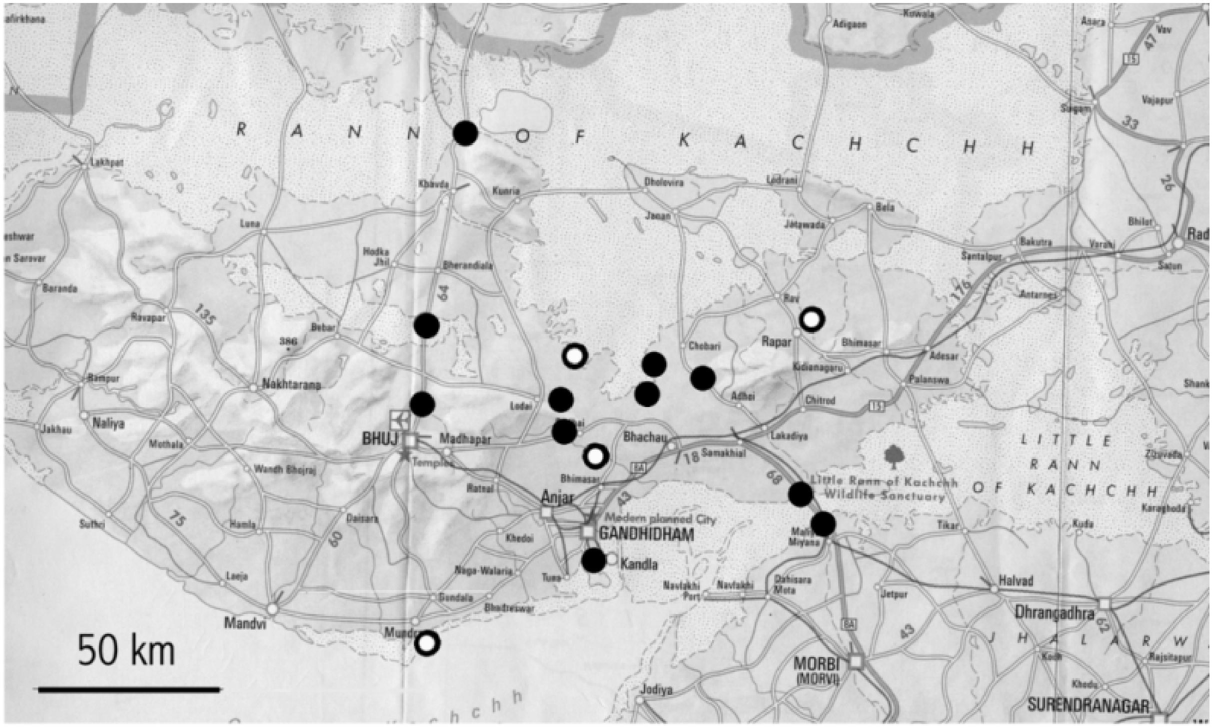

figure 3.1 : Carte de localisation des sites de liquéfaction.
Cercles pleins : sites observés lors de la mission.
Cercles évidés : cas cités par d'autres observateurs.

3.3.1 Liquéfaction

Dans la région du Kachchh, de très nombreuses manifestations de liquéfaction ont été observées sur une vaste zone, et ceci a été signalé par tous les visiteurs du site. Nous avons observé quelques sites où les éjections de sable et d'eau étaient manifestes ; leur répartition (figure 3.1), bien que ne pouvant évidemment prétendre à l'exhaustivité, démontre cependant l'étendue des zones touchées.

Photo 3.5 : Volcans de sable

Photo 3.6 : Venue d'eau et de sable.
Dépôts salins blanchâtres. Alignement sur des fractures

Photo 3.7 : Bourrelet à l'aval d'un glissement horizontal

Photo 3.8 : Fissuration du sol.

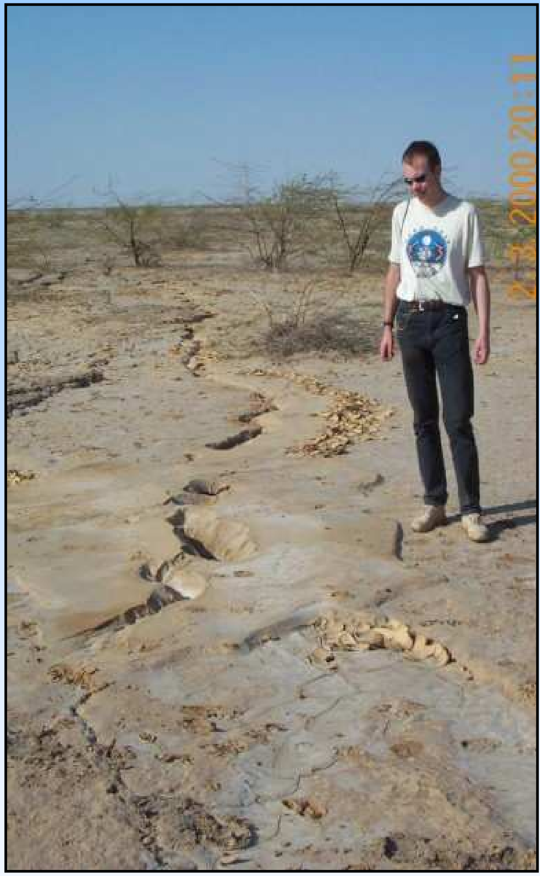

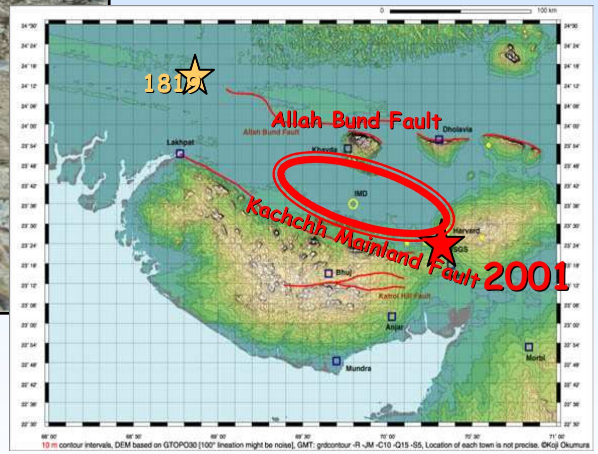

Les taches correspondent aux éjections d'eau (salée) consécutives à la liquéfaction des sables du Rann sur de très grandes surfaces (plusieurs centaines de km²)

De nombreuses traces de liquéfaction sont également présentes

Ejecta le long de fines fissures

Volcan de sable

Ejecta comblant une fissure large

2001 – Bhuj - Inde

Liquéfaction en zones alluviales

Photo 3.10 : Vue générale du barrage sur la rivière Chang

Photo 3.11 : Rupture majeure du corps du barrage. Détail des ruptures côté amont : Avancée du talus et bourrelets émergeant dans le lac.

Photo 3.14 : Rupture du talus amont.
En arrière plan, chute de bloc et
rupture de berge par liquéfaction.

Liquéfaction – Retours d'expériences

5 – Les années 1999-2009

+ Kocaeli (Turquie) -1999,

+ Chi Chi (Taiwan) - 1999,

+ Mise en place d'une grande banque de données par des coopérations US-Turquie et US-Taiwan.
Beaucoup d'essais CPT et les autres, pour comparaisons

+ Workshops US-Japon et US-Taiwan

+ Nombreuses recherches, surtout pour préciser les paramètres de la méthode dite simplifiée et en modélisation :

Fédérateurs de recherches : Idriss, Boulanger, Kramer, Bardet, R. Seed, Cetin, Moss, etc……

+ etc…

CONSTAT GENERAL :

+ Si le phénomène de liquéfaction conduit à un étalement latéral prononcé (# > 1m), il peut y avoir des dommages considérables, aux constructions, mais aussi et surtout aux « réseaux de vie », voies de toutes sortes, canalisations, etc…..

+ Si le phénomène de liquéfaction conduit à des tassements dits post-liquéfaction, car ils peuvent se produire longtemps après la fin du séisme, les constructions vont suivre « gentiment »ces mouvements verticaux et si leur résistance est bonne, cela n’entraine généralement pas de pertes en vie humaine, ce qui est le premier but recherché en génie parasismique.

Attention, malgré tout au comportement des canalisations :

Emploi de polyéthylène à recommander

Liquéfaction – Retours d'expériences

5 – Les années 1999-2009

Disponible en 2009 : **Deux documents de synthèse**

+ I.M. Idriss, R. M. Boulanger : Soil liquefaction during earthquake, Monograph EERI, 2008

+ S. L. Kramer : Evaluation of liquefaction hazards in Washington State, WSDOT, dec. 2008

+ Programme WSLIQ, dérivé de la synthèse de S. L. Kramer, free beta version

Il manque malgré tout à toutes ces études et recherche, une bonne synthèse sur la question majeure : si l''on se trouve devant un problème lié à la liquéfaction possible des sols en présence sur un site, quelle est la meilleure solution à mettre en oeuvre en fonction de nombreuses contraintes :

Voir P. Berthelot et S. Lambert : GT commun AFPS et CFMS

Séismes 2010 :

Ferndale, US – Haïti – Japon – Taiwan - Chili - Turquie,….

Merci de votre attention

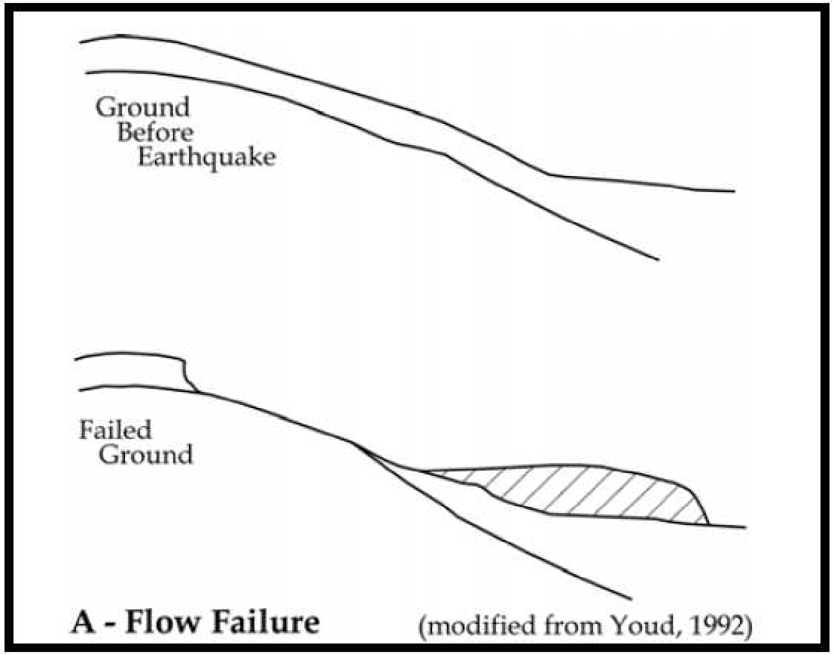
Ground
Before
Earthquake
Failed
Ground
A - Flow Failure
(modified from Youd, 1992)

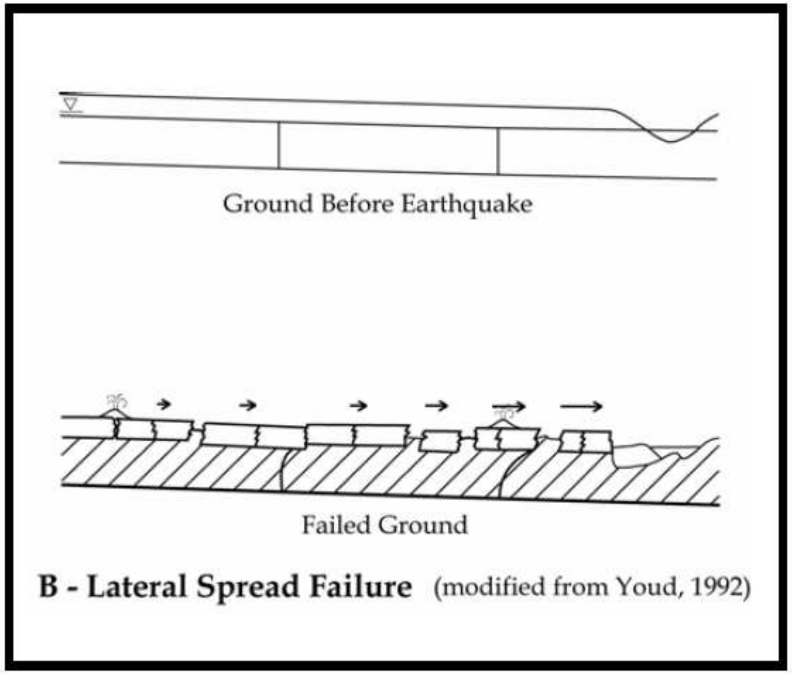
Ground Before Earthquake
Failed Ground
B - Lateral Spread Failure
(modified from Youd, 1992)

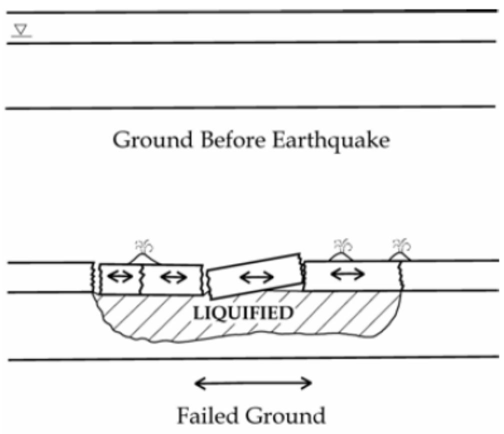

C - Ground Ocillation Failure
(modified from Youd, 1992)

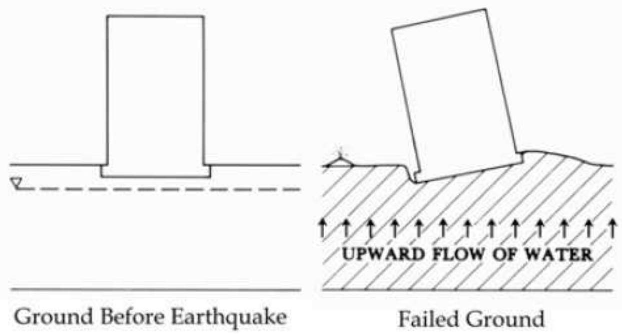

D - Loss of Bearing Strength
(Resulting in Tilted Building and "Floating" Tanks)
(Youd, 1992)

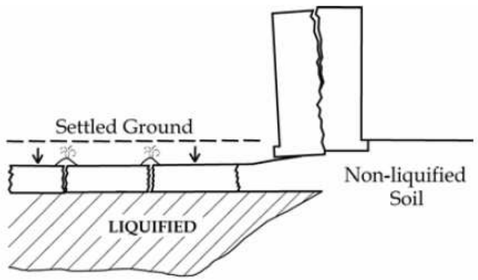

E - Differential Settlement

Runway Program at the San Jose International Airport

SJC is currently extending a shorter runway to create a new full-length runway that should be far less vulnerable to damage because the pavement section is sufficient to "bridge" the stream channels shown as particularly hazardous in the adjacent map. Upon completion of this project, the existing full-length runway will be taken out of service and reconfigured in a similar fashion. Both projects should be completed by 2004.

(M. Wikowski, SJC, personal comm., 2000)

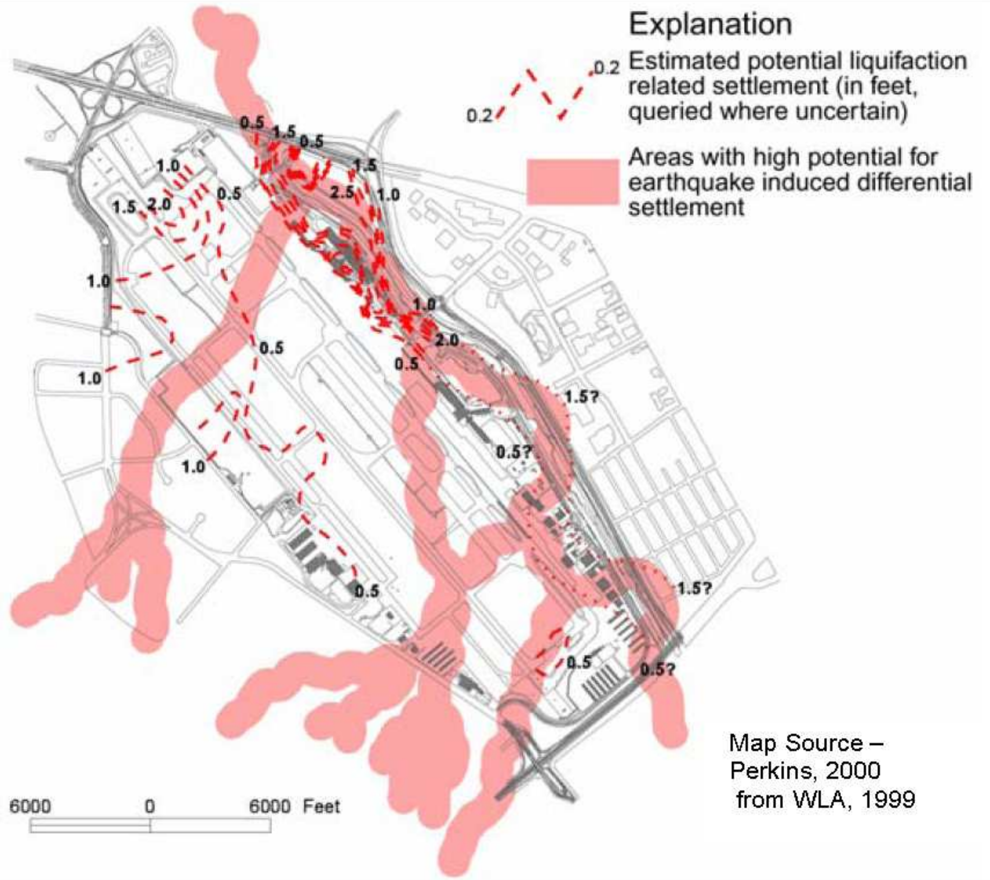

1989 Loma Prieta Earthquake – Port of Oakland
7th Street Marine Terminal
Source – R. Kayen, U.S. Geological Survey and Loma Prieta Collection,
Earthquake Engineering Research Center, University of California, Berkeley

1989 Loma Prieta Earthquake –
Moss Landing Marine Laboratories
Showing structure “stretched” more than 5 feet
due to lateral spreading
Source – L. Harder, Loma Prieta Collection,
Earthquake Engineering Research Center,
University of California, Berkeley

Upper San Leandro Reservoir
showing original hydraulic fill dam
and newer replacement dam
Source – J. Perkins, ABAG